Energy Reports 11 (2024) 1171–1190

Contents lists available at ScienceDirect

Energy Reports

journal homepage: www.elsevier.com/locate/egyr

Research paper

Recent developments in perovskite materials, fabrication techniques, band gap engineering, and the stability of perovskite solar cells

Naveen Kumar Elangovan [a], Raju Kannadasan [a,*], B.B. Beenarani [b], Mohammed H. Alsharif [c], Mun-Kyeom Kim [d,*], Z. Hasan Inamul [e]

[a] Department of Electrical and Electronics Engineering, Sri Venkateswara College of Engineering, Sriperumbudur, Chennai 602117, India
[b] Department of Computer Science and Engineering, Saveetha School of Engineering, Sriperumbudur, Chennai 602105, India
[c] Department of Electrical Engineering, College of Electronics and Information Engineering, Sejong University, 209 Neungdong-ro, Gwangjin-gu, Seoul 05006, the Republic of Korea
[d] School of Energy System Engineering, Chung-Ang University, 84 Heukseok-ro, Dongjak-gu, Seoul 06974, the Republic of Korea
[e] Department of Industrial and Production Engineering, National Institute of Engineering, Mysore 570018, India

ARTICLE INFO

Keywords:
Perovskite materials
Two-step Perovskite deposition
Perovskite solar cells
Device architecture
Band gap engineering
Stability

ABSTRACT

Organic-inorganic hybrid metal halide perovskite solar cells (PSC) represent a novel class of optoelectronic semiconductors that have garnered significant attention from photovoltaic researchers globally. This is due to their continually improving efficiency, straightforward solution processing methods, use of lightweight and cost-effective materials, and other notable features. The advantageous properties of perovskite materials, such as superior charge transport, tunable band gap, and distinctive electronic structure, contribute to their appeal. Over the past 6 to 7 years, diverse device architectures and fabrication techniques for PSC have emerged, achieving an impressive power conversion efficiency (PCE) of 25.7%. This review article primarily focuses on recent advancements in PSC fabrication techniques, synthesis, device architecture, charge transport mechanisms, band gap engineering, and stability. Additionally, it provides a summary of recently reported materials used in various layers of PSC, including the perovskite layer, as well as electron and hole transport layers. Lastly, the article outlines the challenges faced in the development of PSC, offers recommendations, and suggests potential directions for future research to guide the field forward.

1. Introduction

1.1. Background

In the 1950 s, the discovery and development of silicon encouraged research into optoelectronic devices. Various optoelectronic device concepts have been explored based on the development of solar photovoltaic materials such as organic semiconductors, bulk semiconductors, nano-crystalline semiconductors, polycrystalline and amorphous semiconductors. An abrupt rise in the associated technologies has attained efficiency through a detailed comprehend of the underlying fundamentals of working mechanisms and material properties of the related devices. Recent advancements in metal halide semiconductors have been identified as one of the most promising possible light-absorbing materials and excellent charge carrier transport performance, in a broad array of optoelectronic applications, particularly photovoltaic. As a result, tremendous effort has been directed toward developing efficient, low-cost, and environmentally friendly metal halide optoelectronic devices.

The origin of perovskite can be traced back to 1839, when a German scientist named Gustav Rose discovered a novel calcium titanate ($CaTiO_3$) based material in the Ural Mountains and named it "perovskite" after Russian mineralogist Lev von Perovski. The foundation for PSCs is based on Gratzel dye-sensitized solid-state solar cells. The perovskite material was initially employed by Miyasaka in dye-sensitized solar cells as a sensitizer and demonstrated the use of the first $CH_3NH_3PbI_3$ – PSC in 2009 with an efficiency of 3.81% (Kumar and Arumugam, 2020; Kojima et al., 2009). In 2014, it reached 13.2% (Yamada et al., 2014; Green et al., 2019; Wang et al., 2021a; Li et al., 2021a; Elangovan and Arumugam, 2019), and it now has a PCE of 25.2% (Ouedraogo et al., 2020). Due to their rising efficiency, ease of fabrication, low production costs, and excellent optical and electrical

* Corresponding authors.
E-mail addresses: kannadasanr@svce.ac.in (R. Kannadasan), mkim@cau.ac.kr (M.-K. Kim).

https://doi.org/10.1016/j.egyr.2023.12.068
Received 24 January 2023; Received in revised form 20 November 2023; Accepted 30 December 2023
Available online 6 January 2024

properties, PSCs have recently attracted a great deal of research interest. As a significant advancement, the efficiency of tandem perovskite/silicon solar cells achieved a record of 33.7% which was developed by KAUST (KAUST, 2023). Regardless of the incredible power conversion efficiency attained to date, the major obstacles limiting the commercialization of PSCs are material selection, fabrication techniques involved, band gap engineering, hysteresis effect, degradation, and stability issues. These significant obstacles are driving researchers to develop effective PSCs (McGovern et al., 2020; Rahaman et al., 2021; Suresh Kumar and Chandra Babu Naidu, 2021; Elumalai et al., 2016; Mesquita et al., 2018; Hu et al., 2019; Zhao et al., 2018; Wu et al., 2021).

1.2. Recent exploration relating PSCs

Several excellent reviews on the synthesis methods, theoretical analysis, band gap tunability, working mechanism, perovskite materials, and device configurations have previously been articulated and some of the most recent works are discussed below:

In recent years, perovskite solar cells (PSCs) have emerged as a promising technology with the potential to revolutionize the field of photovoltaics. This literature review synthesizes key findings from various studies, highlighting significant advancements and breakthroughs in the development of efficient and stable PSCs. A notable contribution to the field comes from Al-Ashouri et al (Al-Ashouri et al., 2020)., who presented a comprehensive study on monolithic perovskite/silicon tandem solar cells. Their work demonstrated a remarkable efficiency of over 29%, achieved through enhanced hole extraction. This underscores the potential of tandem structures for achieving high conversion efficiencies in PSCs.

In a parallel development, Fehr et al (Fehr et al., 2023). investigated integrated halide perovskite photoelectrochemical cells with solar-driven capabilities. Their research offers insights into the integration of perovskite materials into photoelectrochemical systems, broadening the potential applications of these materials beyond traditional photovoltaics. Addressing concerns related to the environmental impact of electronic devices, the European Commission's directives on the Restriction of Hazardous Substances (RoHS) (European Commission, 2021) highlight the importance of considering the materials used in electronic equipment, including PSCs, to ensure compliance with environmental standards.

Thermochromic properties have also been explored as seen in the work of Cao et al (Cao et al., 2023)., where they investigated stable and rapidly reversible thermochromic behavior in acene alkylamine intercalated layered hybrid perovskites. This research opens avenues for smart window applications with tunable optical properties. Additionally, Rosales et al (Rosales et al., 2023). developed thermochromic halide perovskite windows with ideal transition temperatures, showcasing the potential for efficient energy management in buildings. Furthermore, advancements in stability have been a focal point of recent research efforts. Snaith et al (Snaith et al., 2023a). demonstrated thermally stable PSCs through all-vacuum deposition, offering a pathway for enhanced stability in varying operating conditions. This approach addresses concerns related to the long-term performance of PSCs, a critical factor for their widespread adoption. Another study by Snaith et al (Snaith et al., 2023b). focused on chloride-based additive engineering, contributing to the development of efficient and stable wide-bandgap perovskite solar cells. Their work sheds light on strategies for enhancing both efficiency and stability simultaneously.

In the pursuit of long-term operating stability, Zhu et al (Zhu et al., 2023). conducted a comprehensive review, emphasizing the importance of stability in perovskite photovoltaics. Their work provides insights into the challenges and strategies for achieving stable PSCs over extended periods. Stability is a key consideration for the commercial viability of PSCs, and this review offers a valuable resource for researchers and engineers working in the field. The literature also explores novel applications for integrated perovskite solar cells. Bati et al (Bati et al., 2023). discuss next-generation applications, highlighting the versatility of perovskite materials beyond traditional solar cell configurations. The integration of perovskite solar cells into diverse applications, beyond conventional energy harvesting, signifies the expanding role of these materials in various technological domains. In summary, the reviewed literature showcases the diverse and evolving landscape of perovskite solar cell research. From efficiency enhancements and stability improvements to novel applications and environmental considerations, these studies collectively contribute to advancing the understanding and practical applications of perovskite solar cell technology.

In the following review, we summarise the latest developments in PSC research, which includes a brief description of materials and also the function of various layers in device architectures. We also discuss recent fabrication techniques for improving structural morphology, and band gap engineering for visible light absorption, which improves stability issues and the photo-generation process in PSCs. a quick rundown of the potential and difficulties in passivation technology for improving the performance of PSCs are also presented. This article aims to offer insightful resources for further investigation.

2. Materials

2.1. Perovskite materials

The $CaTiO_3$ compound is the source of the perovskite material, which has a molecular structure of ABX_3. Fig. 1 depicts the elements that make up a perovskite structure with an ABX_3 composition. Perovskite materials have attracted a lot of attention as a result of cubic lattice-nested octahedral structures, and thermal, unique electromagnetic, and optical properties. The following are four characteristics of perovskite materials listed below.

- These materials have high optical absorption coefficients, excellent photoelectric properties, and low exciton binding energy.
- Perovskite can efficiently absorb solar energy.
- The high dielectric constant of perovskite enables efficient photo generation of electrons and holes.
- Electrons and holes are effectively transmitted from 100 nm to more than 1 μm. Such perovskite materials provide significantly short-circuit current densities and open-circuit voltages when employed in solar photovoltaic applications.

To gain a better understanding of the potential and performance of PSCs, a discussion of some perovskite materials is presented. A perovskite solar cell made of methylammonium lead iodide performs very well because of its favorable electronic and optical absorption coefficient properties. The $CH_3NH_3PbI_3$ material-based PSC has an excellent electron mobility of $24.0 \pm 7\ cm^2\ v^{-1}\ s^{-1}$, holes mobility of $105 \pm 35\ cm^2\ v^{-1}s^{-1,}$ and appropriate band gap of 1.55 eV with very good PCE of about 23.7% (Green et al., 2019). Despite the outstanding performance of lead-based PSCs, the toxicity of lead necessitates the alternative development of lead-free PSCs. However, the development of effective encapsulation strategies can reduce Pb exposure. But at the end of the module lifetime, it is important to ensure that all materials have been effectively recycled. Large-scale manufacturing and commercialization of lead-based PSCs may result in the release of Pb into the environment causing significant environmental impact. However, considering the stability of the Pb-based PSC in ambient conditions, it has very low stability (Zimmermann et al., 2016; Zhou et al., 2018; Lekesi et al., 2022; Jiang et al., 2019; Hasan and Joshi, 2022; Joshi et al., 2021; Hasan et al., 2022). To avoid degradation, the whole fabrication process is carried out in a nitrogen gas environment. In this context, development of lead-free PSCs is a challenging factor due to maintenance of stringent criteria to match the optical and electrical properties of lead-halide perovskite. Considered the toxicity and environmental effects of Pb, Y. Li et al. developed a low toxicity perovskite material

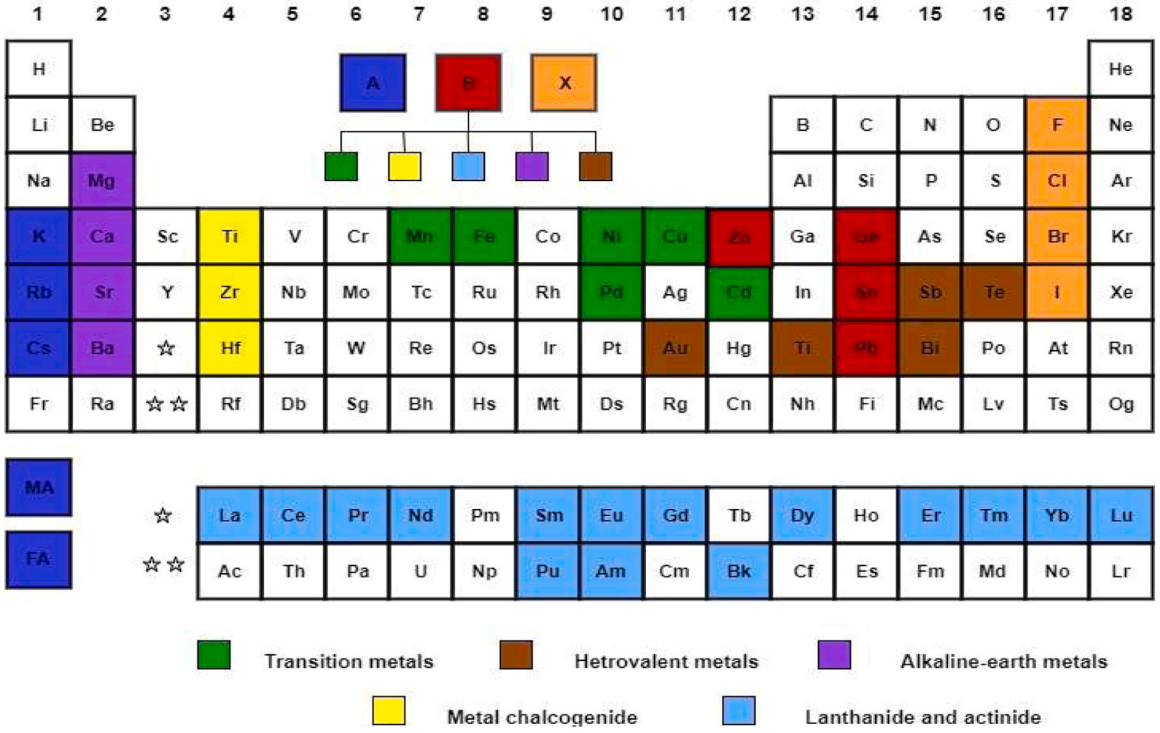

Fig. 1. Perovskite-forming materials with an ABX_3 composition. The organic metal A may be replaced with elements colored dark blue on the periodic table, while the halide ions X = F-, Cl-, Br-, and I- are light brown. Group 14 elements (Sn, Ge), transition metals, the tetravalent substitution of metals, lanthanide, actinide, metal chalcogenides, and alkaline-earth metals are lead replacement elements in perovskite structures.

with a two step spin coating technique that contains 50% Pb and 50% Sn. For the following device configuration ITO/PEDOT:PSS/$CH_3NH_3Sn_{0.5}Pb_{0.5}I_3$/$C_{60}$/Ag, the PSCs demonstrates an efficiency of 13.6% with R_s 5.3 Ω cm^2 (Li et al., 2016a).

According to Krishnamoorthy et al., the most obvious substitute for Pb is the monovalent use of another group 14 metal, such as Ge or Sn, which has a comparable electrical structure to Pb. However, transition metals, lanthanides, and alkaline earth metals can also be taken into consideration as lead replacements (Krishnamoorthy et al., 2015). Germanium iodide perovskite ($MAGeI_3$) has strong potential in photovoltaic applications (Yin et al., 2020), (Chen et al., 2019a). While germanium have very good optoelectronics properties with relatively smooth morphology. The band gap of $MAGeI_3$ ranges from 1.9 to 2 eV (Huang et al., 2021). The device has a photocurrent density of 4 mA/cm^2 and a very strong visible spectrum absorption range. However, the cell's poor performance is caused by the formation of Ge^{4+} ions by oxidation. Improvement of the stability issue and new optimization approaches of germanium perovskite solar cell is currently in the research focus. With a PCE of 5.73% and an ideal band gap of 1.3 eV, the tin halide perovskite device configuration of TiO_2/$CH_3NH_3SnI_3$/Spiro-OMeTAD exhibits improved absorption in the visible spectrum region. However, in contrast to lead perovskite, tin halide perovskite readily oxidizes to the oxidation state Sn^{4+}, resulting in metallic properties and extremely limited atmospheric stability (Hao et al., 2014). By adding pyrazine to the formamidinium tin iodide ($FASnI_3$) solvent solution, an efficiency of 4.8% was achieved while restricting the excessive phase separation brought on by SnF_2 and preventing undesirable Sn^{4+} oxidation. As a possible substitute for lead-free perovskite, bismuth-based perovskite has good optoelectronic characteristics and a tuneable band gap in the visible spectrum. Nevertheless, PSCs using these alternative metal-based perovskites exhibit lower performance compared to their lead-based counterparts. For instance, while $MAPbBr_3$ based perovskite compounds are much more stable under ambient settings than $MAPbI_3$, germanium, and tin-based perovskite materials. This is due to the fact that the degradation of perovskite devices has been linked to the movement of mobile ions (Lee et al., 2016).

$CsPbI_3$-based inorganic lead halide perovskites are now being evolved as a research highlight in the field of PV technology. However, it outperforms hybridorganic–inorganic perovskites concerning thermal stability due to the absence of weakly bonded organic components. Inorganic lead halide perovskites with other compositions, such as $CsPbI_2Br$, $CsPbIBr_2$, and $CsPbBr_3$, have also seen rapid development, with PCE of 9.84% (2016), 17.16% (2020), and 11.53% (2019) respectively. Two significant problems limit the performance of $CsPbI_3$-based PSC. The low tolerance factor causes the preferred phase transformation from perovskite to non-perovskite phase. The second is energy loss due to energy-level mismatch and unavoidable defects, which limits PCE (Liu et al., 2021). M. B. Johansson conducted a thorough investigation into the photo-physical characteristics of perovskites made of $Cs_3Bi_2I_9$ and $CsBi_3I_{10}$. According to the findings, $CsBi_3I_{10}$ has a photocurrent that is larger than that of any other bismuth halide perovskites and a broad spectrum of absorption up to 700 nm (Johansson et al., 2016), (Mariyappan et al., 2020). Chen *et al.*, have fabricated formamidinium lead iodide ($FAPbI_3$) based perovskite solar cells with an efficiency of 19.09% at room temperature. The $FAPbI_3$ material has a narrow band gap, a high light-absorption coefficient, and excellent photo and thermal stability. The narrow band gap $FAPbI_3$ perovskites, on the other hand, are highly desirable for PSCs, which will help to accelerate the commercialization of this promising photovoltaic technology (Chen et al., 2020). Table 1 summarizes the band gap, carrier mobility, and exciton binding energy of various perovskite materials.

2.2. Charge transport layer materials

For the efficient collection of electrons from the conduction band (CB) of the perovskite layer, the typical PSC should contain an electron extraction layer. The electron transport layer (ETL) is a colloidal thin-film made of materials such as TiO_2, SnO_2, ZnO, and CdS or related

Table 1
The band gap, carrier mobility, and exciton binding energy of various perovskite materials are summarized.

Si. No	Perovskite Materials	Bandgap Eg (eV)	Exciton Binding Energy (meV)	Carrier mobility $cm^2\ v^{-1}\ s^{-1}$	Reference
1	$MAPbI_3$	1.55 (tunable)	2-60	$\mu_e \sim 24.0 \pm 6.8$ $\mu_h \sim 105 \pm 35$	(Qaid et al., 2016; Green et al., 2019; Xu and Wang, 2020)
2	$MAPbBr_3$	2.39-2.48	40-150	$\sum = 35$	(Ulatowski et al., 2020; Lee et al., 2016; Krishnan, 2019)
3	$MASnI_3$	1.47-3.54	29	$\mu_e \sim 322$ $\mu_h \sim 2320$	(Bokdam et al., 2016; Hao et al., 2014; Huang et al., 2021)
4	$CsPbBr_3$	2.0	40	$\mu_e \sim 63$ $\mu_h \sim 49$	(Protesescu et al., 2015), (Liu et al., 2021) (Herz, 2017).
5	$CsPbI_3$	1.44	20	$\sum = 33 \pm 5$	(Protesescu et al., 2015), (Liu et al., 2021), (Dastidar et al., 2017).
6	$CsPbCl_3$	2.82	75	$\mu_e \sim 28 \pm 1$ $\mu_h \sim 20 \pm 1$	(Protesescu et al., 2015), (Liu et al., 2021), (He et al., 2021).
7	$FAPbI_3$	1.5	35	$\sum = 27$	(Bokdam et al., 2016; Chen et al., 2020), (Herz, 2017).
8	$FASnI_3$	1.27	31	$\mu_e \sim 103$ $\mu_h \sim 67$	(Bokdam et al., 2016), (Lee et al., 2016), (Huang et al., 2021)

mesoporous systems, with wide grain boundaries and weak recombination at the interface. The porosity, phase, size of the crystalline, and structural morphology of the electron transport layer are the dominant factors that determine the amount of perovskite absorbed on its surface, which can provide perovskite material to enable harvesting photo catalytic activity and improves optoelectronics properties. However, depending on the materials used for the ETL, the PSC may experience UV exposure instability, oxygen vacancy defects, recombination, and inhibiting the photo charge collection (Min Nam et al., 2010; Yang et al., 2015). To address these challenges, several researchers proposed a variety of materials for ETL in PSCs. Regarding this, nano sheets or transition metal with thick atoms such as WS_2, MoS_2, TiS_2, etc have a high potential for use as ETL materials since it is defect-free. MoS_2 is widely used as an ETL in PSC due to its low trap density and thin structure, which improve device stability and facilitate the rapid transportation of charge carriers to the electrode. Furthermore, the device without an electron transport layer reported a very low efficiency of 3.7% and a high series resistance of 79.1 $\Omega\ cm^2$ (Wang et al., 2014). For the collection of the positive charges from the perovskite's valence band, the presence of such an electron transport layer in PSCs is just as crucial as the presence of a hole transport layer (HTL). Moreover, the performance of solar cells is strongly influenced by HTL. To enhance conductivity and suppress charge carrier recombination at the HTL/perovskite interface, much work has been focused on identifying the optimal dopant for HTL. However, PSC without a hole transport layer reported 4.18% of PCE, since there is no inhibition of the electrons' movement towards the back contact, which would otherwise cause a recombination effect (Zhang et al., 2015). Numerous materials, including polymers, Spiro-OMeTAD, organic, and inorganic compounds, have been described in the exploration of hole transport materials for the hole transport layer. The choice of materials for electron and hole transport must take into account many factors. They include the need for very good electron and hole mobility, a functional life span, and an appropriate band gap energy level. In the ideal case, the materials for the charge transport layers should meet the following requirements:

(a) Good charge carrier mobility. As a crucial interfacial layer of perovskite solar cells, charge transport materials play a vital role in electron and hole extraction, transport, and device stability. For the construction of highly efficient and stable PSC, electron and hole transport materials with appropriate energy levels and comprehensive surface passivation effects are required.

(b) Low series resistance R_s. The other factor which influences the performance of the PSC was the series resistance R_s. Series resistance and the recombination effect are increased as a result of the thick electron and hole transport layer. The series resistance, short circuit current leakage, and pin-holes are decreased with an improvement in charge mobility and conductivity by adjusting the layer thickness. Inappropriate device construction, subpar film quality, and unsuitable surface coverage of the electron, perovskite, and hole transport layers were other significant causes of series resistance.

(c) Energy level. Energy band alignment controls charge transport and separation in perovskite solar cells. The valence band of the hole transport layer should coincide with the HOMO level of the perovskite film. Similar to this, the CB of the electron transport layer should match up with the LUMO level of the perovskite.

However, the current study summarises a brief description of various electron and hole transport materials for PSC reported recently. The unique property of perovskite material made the choice of electron transport material more critical. Xin Li *et al.*, fabricated TiO_2-nanorod for analyzing the performance of the PSC. The results reported in their study showed a greater potential in power conversion efficiency for the TiO_2-nanorod-based electron transport layer due to its faster electron extraction and an open structure than the TiO_2 mesoporous film. However, the synthesized TiO_2-nanorod array with the capped and uncapped structure for perovskite solar cell application exhibited a difference in the device performance. The capping layer eliminates direct contact of the TiO_2-nanorod layer with the hole transport layer TiO_2-nanorod array with the capping layer for PSC exhibited a 13.80% of PCE over the TiO_2-nanorod with uncapping layer (Li et al., 2016b).

Acik *et al.* fabricated a 0.10% wt single-walled carbon nanotube with nano-crystalline TiO_2 photo electrodes for perovskite solar cell applications. Furthermore, they discovered a considerable improvement in the electron transport layer as a result of appropriate band energy alignment and a reduced charge recombination effect, which increased the power conversion efficiency to 16.11% (Acik and Darling, 2016). The use of carbon nano-tube-based TiO_2 was also found to reduce the anomalous hysteresis J-V behavior due to the reduced series resistance (Mariyappan et al., 2020; Batmunkh et al., 2017), developed a graphene/TiO_2 as ETL for the PSC application. The results showed employing graphene with TiO_2 enhances the electron conductivity resulting in increasing PCE in the perovskite solar cell. Zinc oxide (ZnO) was considered the potential ETL in addition to titanium dioxide film due to its matching band structure, transparent, higher electron mobility (230 $cm^2\ v^{-1}\ s^{-1}$) and ZnO also has a lower sintering temperature than TiO_2. However, when it comes to solar cell devices, the stability of PSCs based on ZnO and TiO_2 lags behind.

Tong *et al.*, fabricated a CdS-based flexible PSC with the following device architecture, namely FTO/CdS/$CH_3NH_3PbI_3$/Spiro-OMeTAD/Ag using the chemical vapor deposition method. Due to its enhanced hole mobility and reduced series resistance, Spiro-performance OMeTAD concerning hole transport material has shown an amazing performance for PSC application. The results indicated the thickness of the electron transport layer ranging from 30 to 120 nm with an increase in power conversion efficiency till 50 nm and a further increase in electron transport layer thickness above 100 nm there was a decrease in efficiency as clearly identified. This is due to the increase in the thickness of

ETL increasing the series resistance (8.6 Ω cm^2) of the device which resulted in a decrease in PCE. The thicker CdS layer transmitted photons of a smaller number to the perovskite layer which results in fewer generations of electron-hole pairs. PCE of up to 14.68%, Jsc of 20.76 mA/cm^2, Voc of 1.04 V, and FF of 68% was achieved for the following device structure (Tong et al., 2017). However, the device with good crystallinity, smoother morphology, and reduced porous size causes the series resistance of the electron transport layer to drop. This line of action results in an increased flow of electrons, and as a result, the power conversion efficiency of PSC increases. Fig. 2 depicts the effect of the series resistance of various electron transport materials on the performance of a perovskite solar cell. Abulikemu *et al.* studied the effect of SnO_2/CdS ETL in their examination of the performance of $CH_3NH_3PbI_3$-based PSCs. A quantitative correlation was performed for SnO_2 and SnO_2/CdS-based PSC fabricated using the spin coating method (Abulikemu et al., 2017) (Mohamadkhani et al., 2019). Non-stoichiometric flaws, including oxygen vacancies, and significant light instability difficulties over continuous illumination revealed CdS thin film to be the superior substitute for TiO_2 and ZnO electron transport material for PSC. And also, maximum efficiency in fact reached for the device fabricated using TiO_2-based perovskite solar cells.

CdS a non-oxide metal chalcogenide is an outstanding semiconductor material with a direct band gap, high optical properties, high stability, appropriate energy band gap, low-temperature fabrication material, and excellent electron mobility of (~ 10 cm^2 V/s). Hence it was found to be a good replacement for utilizing CdS as electron transport material for the fabrication of PSC. The results showed a greater PCE of 17.18% by the cell fabricated using SnO_2/CdS than the cell fabricated using SnO_2 with an efficiency of 15%. This is due to improved PL quenching caused by the CdS layer, which results in improved electron transport and collection from the perovskite layer. On the other hand, the cell fabricated using SnO_2 showed a high hysteresis index of 0.17 and for SnO_2/CdS-based device has a lesser hysteresis index of 0.05 which ultimately resulted in better efficiency. However, employing a CdS layer between SnO_2 and perovskite layers resulted in a decrease in charge accumulation and enhanced charge transportation at the interface between electron transport and the perovskite layer.

Kim *et al.,* have performed a comparative analysis of rutile SnO_2/$MAPbI_3$ and rutile TiO_2/$MAPbI_3$ interfaces to investigate the performance of perovskite solar cells. SnO_2/$MAPbI_3$ outperforms TiO_2/$MAPbI_3$ in terms of band alignments, suppression of mid-gap defect states, and massive electron carrier injection. The findings show that SnO_2 has better band alignments to $MAPbI_3$ at both MAI and PbI_2 terminations than typical TiO_2. Because of significant orbital hybridizations, the carrier injection of SnO_2/$MAPbI_3$ is greater than that of TiO_2/$MAPbI_3$. Unlike the TiO_2 interface, the interfacial defect levels of SnO_2 do not generate deep recombination effects. This feature of the electron transfer mechanism in the SnO_2/$MAPbI_3$ interface may pave the way for enhanced performance in PSCs (Kim et al., 2020).

Wang *et al.*, have examined the impact of $Ti_3C_2T_x$ MXene electron transport material on the performance of PSCs concerning configuration ITO/MXene/Perovskite/Spiro-OMeTAD/Au. $Ti_3C_2T_x$ MXene, a two-dimensional electron transport material with high transparency, high conductivity, tuneable binding energy, and functional quality, has attracted the curiosity of researchers in PSCs. The $Ti_3C_2T_x$ MXene-based PSCs outperform in terms of device stability, the current density of 21.5 mA/cm^2, and PCE of 18.9% (Wang et al., 2021b). Despite the excellent material properties of MXene-based PSC, performance is still inferior to that of classic TiO_2 or SnO_2-based PSCs. Patil *et al.*, have studied the effect of PCBM, or [6,6]-phenyl C61 butyric acid methyl ester, a fullerene derivative as an electron transport material in inverted perovskite solar cells with the device configuration of ITO/NiO/Perovskite/ PCBM-SnS_2/ZnO/Ag. Nevertheless, difficulties at the perovskite/PCBM interface, such as inefficient electron transportation, a large electron trap zone, poor film production, and abundant non-radiative recombination, cause the inverted perovskite solar cell's performance to be relatively poor. To address these issues, a homogeneous combination of PCBM-SnS_2 is used as the ETL, resulting in high

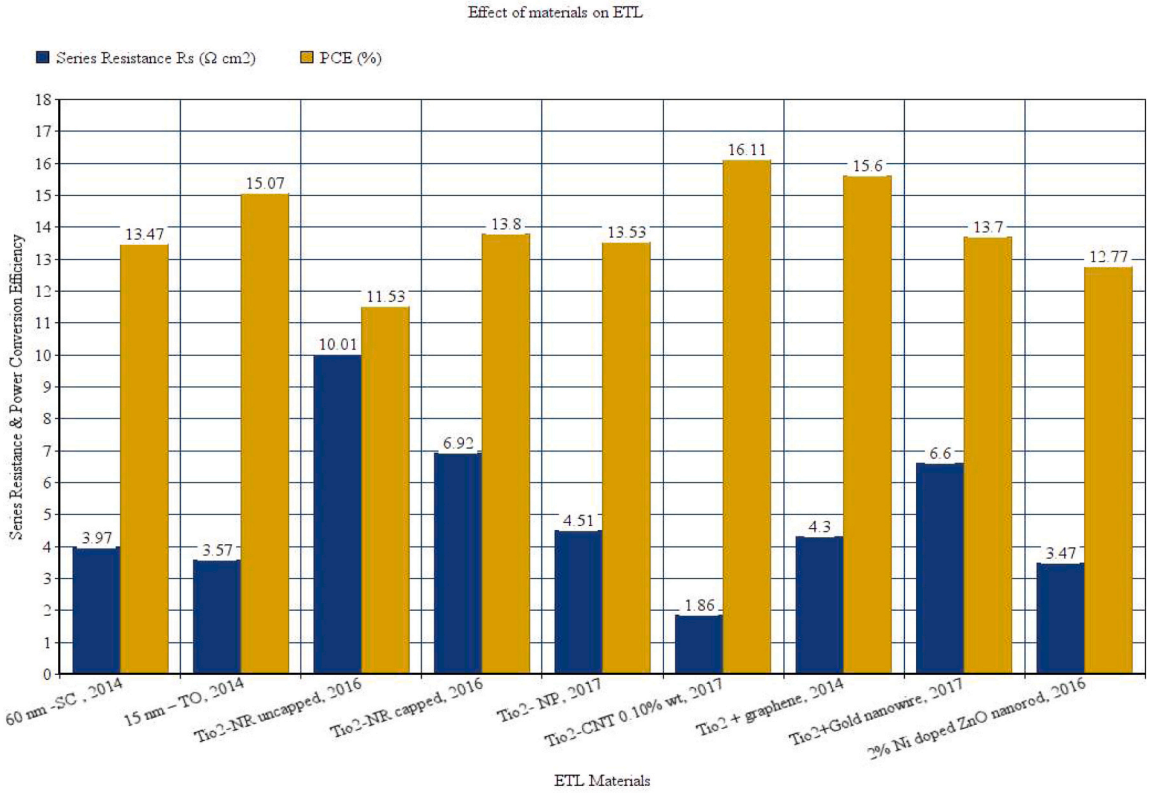

Fig. 2. Influence of series resistance on perovskite solar cell performance.

electron transit and favorable energy levels. Furthermore, due to SnS_2's higher relative permittivity, the crucial electron captured radius reduced from 0.62 nm to 0.22 nm, lowering leakage current and non-radiative recombination at the perovskite/PCBM-SnS_2 interface. Following this, the PSC based on PCBM-SnS_2 exhibited a better PCE of 19.95% than the device based on PCBM, which demonstrated a PCE of 18.22% (Patil et al., 2020). Table 2 summarises the influence of various electron and hole materials on the performance of PSC.

3. Fabrication techniques and their influences

3.1. Perovskite fabrication techniques

The formation of hybrid organic-inorganic metal halide perovskite crystals is a simple stoichiometry reaction. Nevertheless, most research focused on improving perovskite quality by adjusting process parameters such as precursor solution concentration ratios, temperature, and fabrication techniques, all of which appear to have a substantial effect on the formation of perovskite thin film. Nevertheless, perovskite film quality has a strong influence on PSC performance, as high-quality perovskite film attributes to better light absorption, negligible charge recombination, and long carrier diffusion length. As a result, there is no doubt that enhancing the perovskite film quality is one way to improve PSC performance. To develop perovskite, synthesis factors including temperature, concentration, precursors, solvent, surfactant, atmosphere, time, flow rate, and distribution rate must be monitored. On the other hand, controlling the growth of perovskite on various substrates is crucial for producing high-quality films with large grains, high crystallinity, and smooth surfaces. For the fabrication of perovskite thin film, the choice of deposition method is more important for improving structural morphology. One-step deposition, two-step spin coating deposition, two-source vapour deposition, sequential vapour deposition, and vapour-assisted solution deposition are some of the deposition processes utilized for perovskite. In Table 3, typical perovskite thin film deposition processes are compared.

3.2. The influence of precursor concentration on the perovskite film quality

Various perovskite materials have been used as active layers in PSCs to date. Nevertheless, we have only summarised recent work on the influence of precursor concentration ratios on methylammonium lead iodide ($MAPbI_3$) based perovskite film due to its superior electrical and optical properties when compared to other perovskites. The majority of

Table 2
Influence of materials on perovskite solar cell performance.

SI. NO	Materials	Voc (V)	Jsc (mA cm^{-2})	FF	PCE (%)	Remarks	Reference
1.	**TiO_2 15 nm Thermal Oxidation**	1.09	21.97	0.63	15.07	Thermally oxidized TiO2 compact film possesses a high short-circuit current density, high PCE, and a uniform surface with Rs of 3.57 (cm^2).	(Ke et al., 2014)
2.	**TiO_2-NR capped**	1.02	20.1	0.671	13.80	TiO_2-Nanorods with a capping layer prevent electron-hole transport material from contacting which results in a decrease of series resistance R_s of 6.92 (Ω cm^2) and stimulates increases in PCE.	(Li et al., 2016b)
3.	**TiO_2-CNT 0.10% wt**	1.041	21.96	0.7	16.11	TiO_2-CNT improves the electron transfer rate. This enhancement in electron transport characteristics is projected to reduce charge recombination and series resistance Rs to 1.86 (Ω cm^2) and improve PCE.	(Batmunkh et al., 2017)
4.	**Graphene + TiO_2**	1.04	21.9	0.73	15.6	Graphene + TiO_2 offers better charge mobility, lower series resistance Rs of 4.3 (Ω cm^2), and increased conductivity.	(Wang et al., 2014)
5.	**No electron Transport layer**	0.95	10.8	0.37	3.7	The absence of ETL series resistance increases Rs to 79.1 (Ω cm^2), decreasing efficiency.	(Wang et al., 2014)
6.	**ZnO**	1.01	20.5	0.69	14.4	Better electron mobility than Al_2O_3 and TiO_2. However, stability is lower than TiO_2/PSC.	(Liu and Kelly, 2014)
7.	**2% Ni + ZnO NR**	0.81	23.18	0.68	12.77	Metal-doped ZnO increases visible light photo catalysis and photo production, while nanorod arrangement reduces Rs of 3.47 (Ω cm^2) and recombination impact.	(Dong et al., 2014)
8.	**5%Al + ZnO**	0.9	19.77	0.6	10.7	Al interfacial layer reduces charge recombination and boosts photogeneration.	(Chen and Yang, 2016)
9.	**SnO_2/one-step perovskite**	1.07	20.02	0.48	10.27	One-step XRD peaks are miscellaneous and degraded I_2 is absorbed with a high series resistance of R_s of 22.5 (Ω cm^2)	(Wang et al., 2018a)
10.	**SnO_2/two-step perovskite**	1.0	20.86	0.77	16.11	Film fabricated using the two-step method show perfect and pure perovskite XRD peaks with low series resistance R_s of 3 (Ω cm^2) and also enhanced PCE.	(Wang et al., 2018a)
11.	**CdS-ETL**	1.04	20.76	0.68	14.68	Optimizing CdS layer thickness to 50 nm reduces series resistance R_s of 8.6 (Ω cm^2) with improved power conversion efficiency.	(Tong et al., 2017)
13.	**TiO_2/$MAPbI_3$/Py-C**	0.89	20.2	0.69	12.4	Arylamines with a pyrene core are less expensive than Spiro-OMeTAD and also have a reduced series resistance of 5.157 Ω cm^2.	(Jeon et al., 2013)
14.	**FTO/ TiO_2/ $CH_3NH_3PbI_3$/CuI/Au**	0.62	18.9	0.71	8.3	Lower open circuit voltage, sustained for 54 days without encapsulation, stronger electrical conductivity than Spiro-OMeTAD.	(Christians et al., 2014)
15.	**FTO/Al_2O_3/$CH_3NH_3PbI_2Cl$/ Spiro-OMeTAD/Ag**	0.98	17.8	0.63	10.9	High-hole mobility, low-series resistance, and expensive material.	(Lee et al., 2012)
16.	**TiO_2/$MAPBI_3$/*po*-Spiro-OMeTAD/Au**	1.0	21.2	0.7	16.7	Better band gap energy, lower series resistance of 3.29 Ω $cm^{2,}$ and high shunt resistance result increase in efficiency.	(Jeon et al., 2014)
17.	**FTO/ TiO_2/ $CH_3NH_3PbI_3$/H101/ Au**	1.04	20.5	0.65	13.8	FK102 chemically doping with H101 reduces the Fermi level and improves charge mobility and performance.	(Li et al., 2014)
18.	**FTO/ZnO/ $CH_3NH_3PbI_3$/carbon**	0.73	24.74	0.82	15.02	Tuning the dopant concentration to the energy level of perovskite and electron transport material strongly influences perovskite solar cell performance.	(Lin et al., 2017)
19.	**FTO/compact-TiO_2/TiO_2 nanowire/$CH_3NH_3PbI_3$/Spiro-OMeTAD/Au**	1.23	19.5	0.81	19.5	Nanowire promotes greater charge transportation by suppressing the series resistance and recombination effect. A thicker electron transport layer promotes weaker photon absorption to the perovskite layer.	(Wu et al., 2016)
20.	**TiO_2/ZrO_2/ CH3NH3PbI3/ carbon**	0.91	21.40	0.65	12.77	The study shows that the accumulation of charges at the interfaces, recombination of charges, and ion migration are the important factors causing the hysteresis effect which results in a decrease in PCE.	(Wu et al., 2016)

Table 3
The most common perovskite thin film fabrication techniques.

SI. No	Methods	Description	Advantages	Disadvantages	Stability	Reference
1	one-step deposition	To form perovskite, a solution containing both organic and inorganic materials is spin-coated on a substrate and afterward annealed.	Cost-effective, simple to implement, and fast process.	Poor film quality reduces efficiency, and the choice of a solvent that can dissolve both components at the same time is limited.	MPPT power conversion efficiency was stabilized for 250 s	(Li et al., 2016c)
2	two-step spin coating deposition	First, an inorganic component solution is spin-coated on a substrate, followed by an organic component solution spin-coating and annealing.	It has greater control over crystal formation and growth, is more cost-effective, and has superior photovoltaic performance when compared to other methods.	Preparation takes time. PbI_2 traces were observed in the final perovskite. When compared to vacuum processes, there is less control over film thickness.	At 45 °C and 1 sun, it maintained more than 80% of its initial PCE for 500 h.	Elumalai et al. (2016)
3	sequential vapour deposition	To make perovskite, a bi-layer film of inorganic and organic components is sequentially deposited, followed by thermal annealing.	Removes the drawbacks of the one-step deposition method.	The vacuum process, requires high energy, limiting mass production and costs. Requirements for a high vacuum and temperature.	After 100 h of continuous illumination, the PCE remained at 90% of its initial value.	(Zhao and Zhu, 2015)
4	two sources vapour deposition	Perovskite is formed by co-evaporating organic and inorganic components and then annealing them.	Higher efficiencies are due to better film uniformity than solution processes. Less variation in thickness than in simple solution-processed layers.	The vacuum process consumes a lot of energy and it is difficult to control both component deposition rates. Requirements for a high vacuum and temperature.	After 62 days at room temperature, the degradation rate was 9%	(Zimmermann et al., 2016)
5	vapour assisted solution deposition	Spin-coating is used to deposit an inorganic component, which is then exposed to the organic component's vapour at a high temperature.	The combination of vapour and solution-based processes produces higher-quality films. Low demand for vacuum and temperature required. Well-defined grains.	The vacuum process necessitates a lot of energy. It takes tens of hours for the gas–solid reaction to complete full conversion.	After 14 days (without encapsulation) in the air at 50% RH and 20 °C, there were no traces of PbI_2 in the device.	(Qin et al., 2014)

$MAPbI_3$ perovskite thin films reported are prepared using a two-step deposition technique. However, the composition of the precursor concentration solution, on the other hand, is crucial in solution processing. Because of its high stoichiometric and surface defect tolerance factors during the fabrication process, the electronic structure of $MAPbI_3$ is insensitive to a wide range of compositional changes. Nevertheless, it is unclear whether an excess of MAI or PbI_2 precursor solution is beneficial for enhancing the performance of perovskite materials. Furthermore, researchers have also proposed various types of mechanisms that are responsible for the significant improvement. The concentration of the precursor solution is essential for controlling the crystallinity, morphology, and colloidal nature of halide perovskites. The existing colloidal particles act as nucleation sites during the preparation of perovskite films from their precursors, thereby affecting the quality of the films. Hong, Xie, and Tian *et al.,* created $MAPbI_3$ films by carefully adjusting the MAI and PbI_2 ratios under either I-rich or Pb-rich conditions, and discovered that solvent engineering and stoichiometric affected the efficiency, photo-stability, surface morphology, and coverage ratio of $MAPbI_3$ films (Hong et al., 2021). On the other hand, adding excess MAI to the precursor solution, and depositing with a Lewis acid-base adduct, effectively suppresses non-radiative recombination at grain boundaries (Son et al., 2016). According to Chen *et al.,* releasing the organic species during annealing allows the PbI_2 phase to be present in the perovskite grain boundaries, which can result in improved carrier behavior and carrier stability (Chen et al., 2014). Furthermore, the findings demonstrated that DMF is a good solvent for PbI_2 and MAI, which can control the crystallization velocity and thus aid in the formation of the compact perovskite film (Chen et al., 2019b). Wieghold *et al.* affirmed that higher precursor concentrations contributed to larger and more oriented grains of $MAPbI_3$ films (Wieghold et al., 2018). Park BW *et al.*, demonstrated how the existence of surplus lead iodide in perovskite precursor solution was essential for exceeding 20% power conversion efficiency by reducing halide vacancy (Suresh Kumar and Chandra Babu Naidu, 2021).

Hasan et. al. investigated the perovskite material (PbI_2 and MAI diffused layer) using a synchrotron source-based XRD instrument with different incidence angles for different ratios by varying both the PbI_2 and MAI component within the perovskite material. In his studies, he found that the ratio 1:1 (PbI_2/MAI) shows the better inter diffusion of both PbI_2 and MAI to form fully converted perovskite material, which this full conversion ultimately helps in better chemical bonding and better stability. The XRD curve of a PbI_2 thin film on a bare ITO substrate with an angle of incidence of $\alpha_i = 0.14^\circ$ is shown in Fig. 3(a). Fig. 3(b-d) displays the XRD scans of perovskite films for three distinct molar ratios of PbI_2/MAI at angles of incidence of 0.07°, 0.12°, and 0.14°. The XRD scans of the perovskite layer over ITO for the varied ratios are shown in Fig. 4(a–c) (Hasan and Joshi, 2022; Joshi et al., 2021; Hasan et al., 2022).

Bahtiar *et al.,* fabricated a PSC with the corresponding device structure FTO/PEDOT: PSS/$CH_3NH_3PbI_3$ using the sequential deposition method. According to the study results, two-step perovskite deposition has a substantial effect on the performance and structural properties of perovskite solar cells. In this process, the PbI_2 precursor solution was made using 900 mg of PbI_2 + 2 ml of DMF solution stirred together continuously at 70 ℃ for 24 hrs. Once the solution was prepared, it was spin-coated above the PEDOT: PSS at different rpm, annealing temperature, and annealing time. Then, after the MAI precursor solution was prepared using 90 mg of MAI in 2 ml of IPA, and once the precursor solution was made, it was spin-coated above the PbI_2 layer. Single-step spin coating enhanced PEDOT: PSS surface morphology and decreased pinholes, increasing power conversion efficiency. The results indicated the prepared perovskite at a specific spin coating rpm of 1000 for 20 s, for the specific annealing temperature of 40 ℃ and 100 ℃, and for the specific annealing time at 180 s and 300 s, showing better structural properties with pin hole free surface and also large grain size above 500 nm is obtained in this study (Bahtiar et al., 2017).

Minhuan Wang *et al.* studied the differences between the one-step and two-step deposition methods for analyzing the performance of $CH_3NH_3PbI_3$-based perovskite. In this process, a one-step perovskite precursor solution was made by adding both PbI_2 and MAI in the DMF+DMSO solution with a volume ration of 1:4. The precursor solution was made at one-step, it was directly spin-coated above the substrate at an rpm of 3000 for 50 s. However, in the two-step process, PbI_2

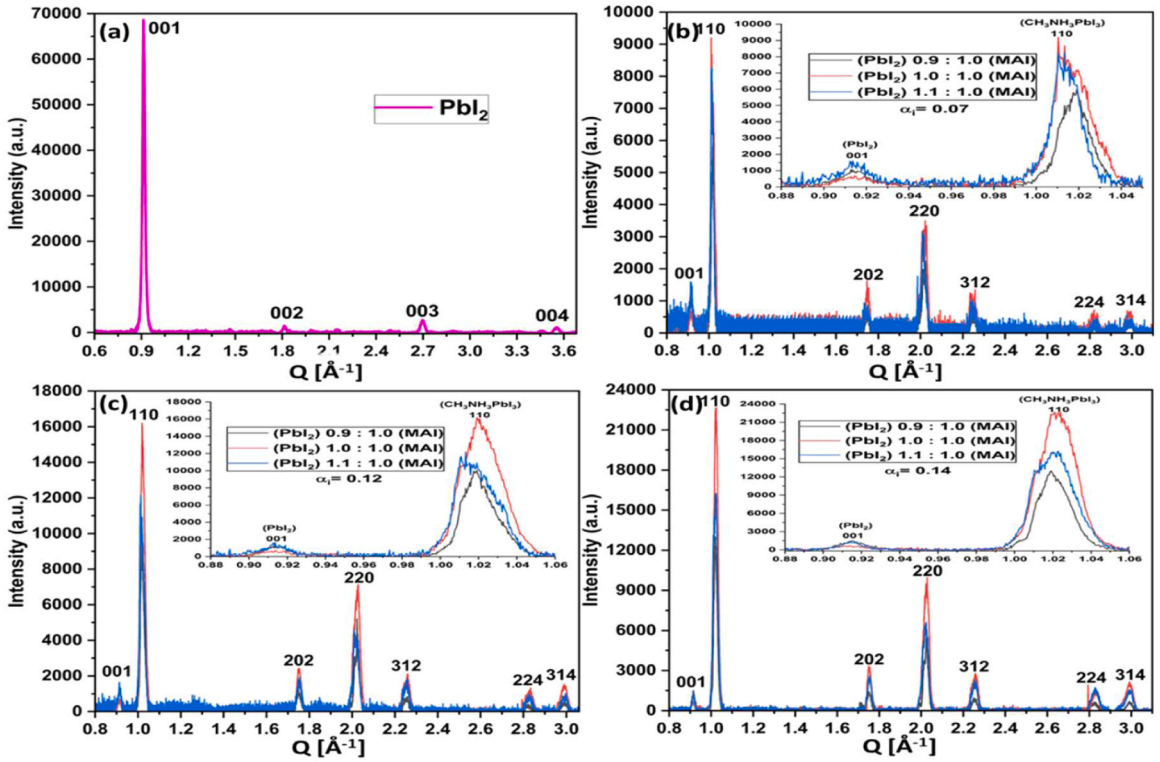

Fig. 3. (a) Out-of-plane scan of PbI_2 layer, (b), (c) & (d) Out-of-plane XRD scan of perovskite layer of changing PbI_2 ratio at an angle of incidence of 0.07°, 0.12°, and 0.14°. Permission to reprint (Hasan and Joshi, 2022).

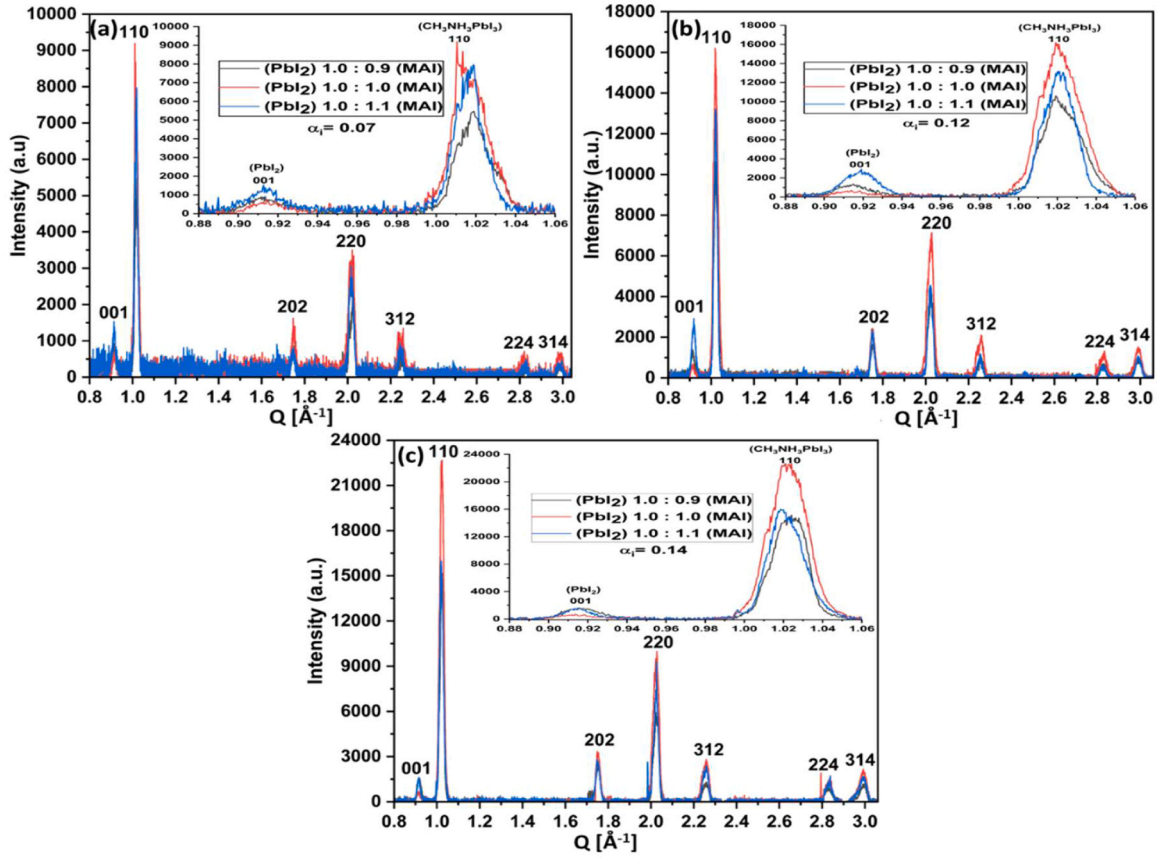

Fig. 4. Out-of-plane XRD scan of changing MAI ratio of the perovskite layer. (a) at an angle of incidence $\alpha_i = 0.07°$, (b) $\alpha_i = 0.12°$, (c) $\alpha_i = 0.14°$. Reprinted with permission from (Hasan and Joshi, 2022).

was spin-coated first at an rpm of 5000 for 5 s followed by MAI solution at 500 rpm for 30 s and finally, it was annealed at 150 ℃ for 20 mins. The XRD results indicated the film was fabricated using a two-step method showing perfect and pure perovskite peaks. While one step XRD peaks were miscellaneous and degraded I_2 was absorbed. However, the SEM image confirmed than one step method of perovskite fabrication two-step method to be having better structural properties with no pin-holes, and dense coverage which resulting in minimized leakage current by enhancing the PCE in perovskite solar cells (Wang et al., 2018a; Liu et al., 2020).

Liu *et al.* fabricated a PSC with the device architecture ITO/ZnO/$CH_3NH_3PbI_3$/P3HT/Ag through two-step spin coating and thermal deposition methods for the examination of the influence of perovskite layer thickness on the performance of PSC. The results indicated the thickness of the perovskite layer ranging from 100 to 600 nm having an increase in PCE till 330 nm and further increase of perovskite layer thickness above 400 nm there is a decrease in efficiency as clearly identified. For the optimum perovskite layer thickness of 330 nm, the PSC device exhibits an efficiency of 11.3% for thermal deposition and 11.8% for the sequential deposition method. For the thickest $CH_3NH_3PbI_3$ film, the deposition of P3HT polymer hole transport material had trouble penetrating the perovskite surface which could cause increased series resistance in the device causing a decrease in power conversion efficiency (Liu et al., 2014). Furthermore, many findings have been reported on the approach of various precursor concentrations using a sequential deposition method in which PbI_2 is spin-coated first and MAI is introduced later. However, the various other reported methods of perovskite synthesis methods are depicted in Fig. 5.

According to the reported literature studies, the two-step sequential deposition method of perovskite formation has greater control over crystal formation and growth is more cost-effective and has superior photovoltaic performance when compared to all other methods. Fig. 6 depicts the most common fabrication methods for perovskite thin film.

3.3. Charge transport layer fabrication issues

The selection of fabrication techniques is the primary goal of PV device manufacturing. Manufacturing technique has an impact on layer roughness, surface morphology, electrical properties, and device performance. So far, many findings have been reported on the approach of various deposition techniques for charge transport layers. This article, on the other hand, discusses some of the most recently reported fabrication techniques for charge transport layers to boost perovskite solar cells' performance. Ke *et al.* examined the impact of the electron transport layer deposition technique on the performance of PSCs. A quantitative correlation was performed simultaneously for the thermal oxidation and spin coating method for the fabrication of TiO_2 compact and mesoporous ETL. The results showed the cell fabricated using thermal oxidation as much thinner than that fabricated using the spin coating method, leading to a reduced recombination effect, low series resistance, and increased charge transfer property. Furthermore, it is examined that thinner TiO_2 film results in greater light absorption for the perovskite film than the thicker TiO_2 film. Hence, optimization of the thickness of the electron transport layer was seen as having an impact on the performance of the PSC. However, the TiO_2 film fabricated using the spin coating method had a thickness of 60 nm and the PCE was estimated to be 13.47%. The TiO_2 film fabricated using the thermal oxidation method had a thickness of 15 nm and the PCE is estimated to be 15.07% (Ke et al., 2014).

Rong *et al.*, have fabricated printable PSC for the triple layer TiO_2/

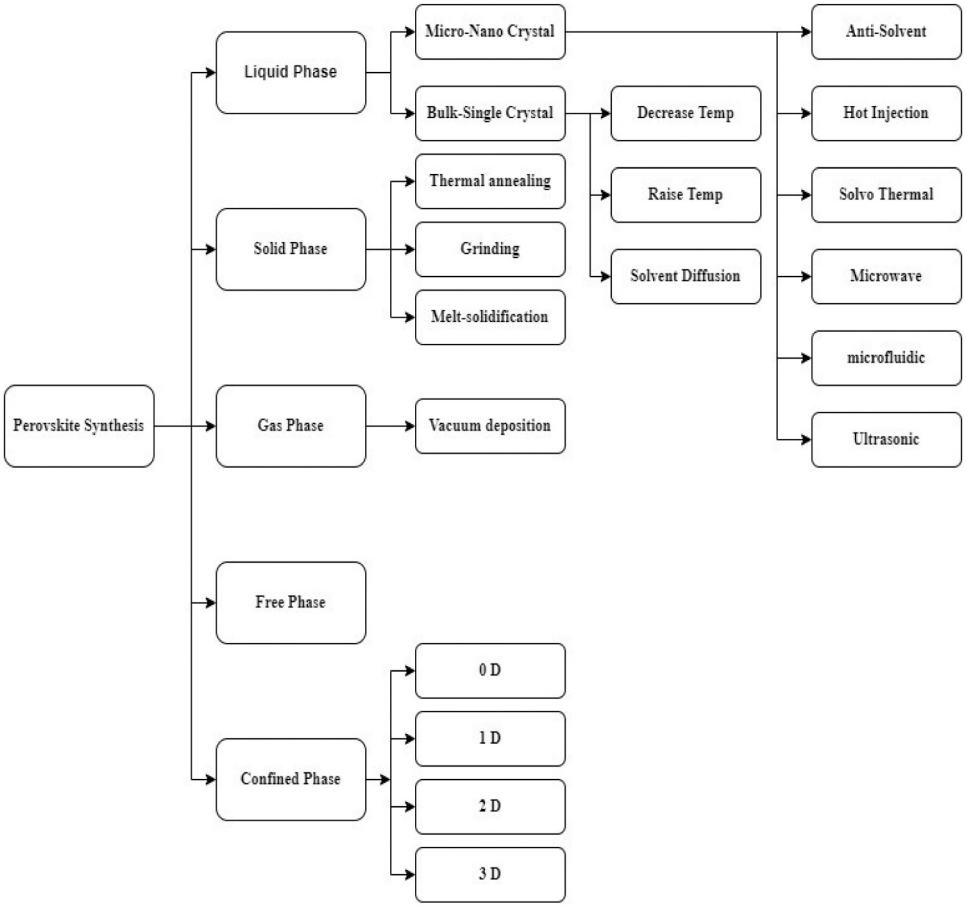

Fig. 5. Perovskite synthesis methods.

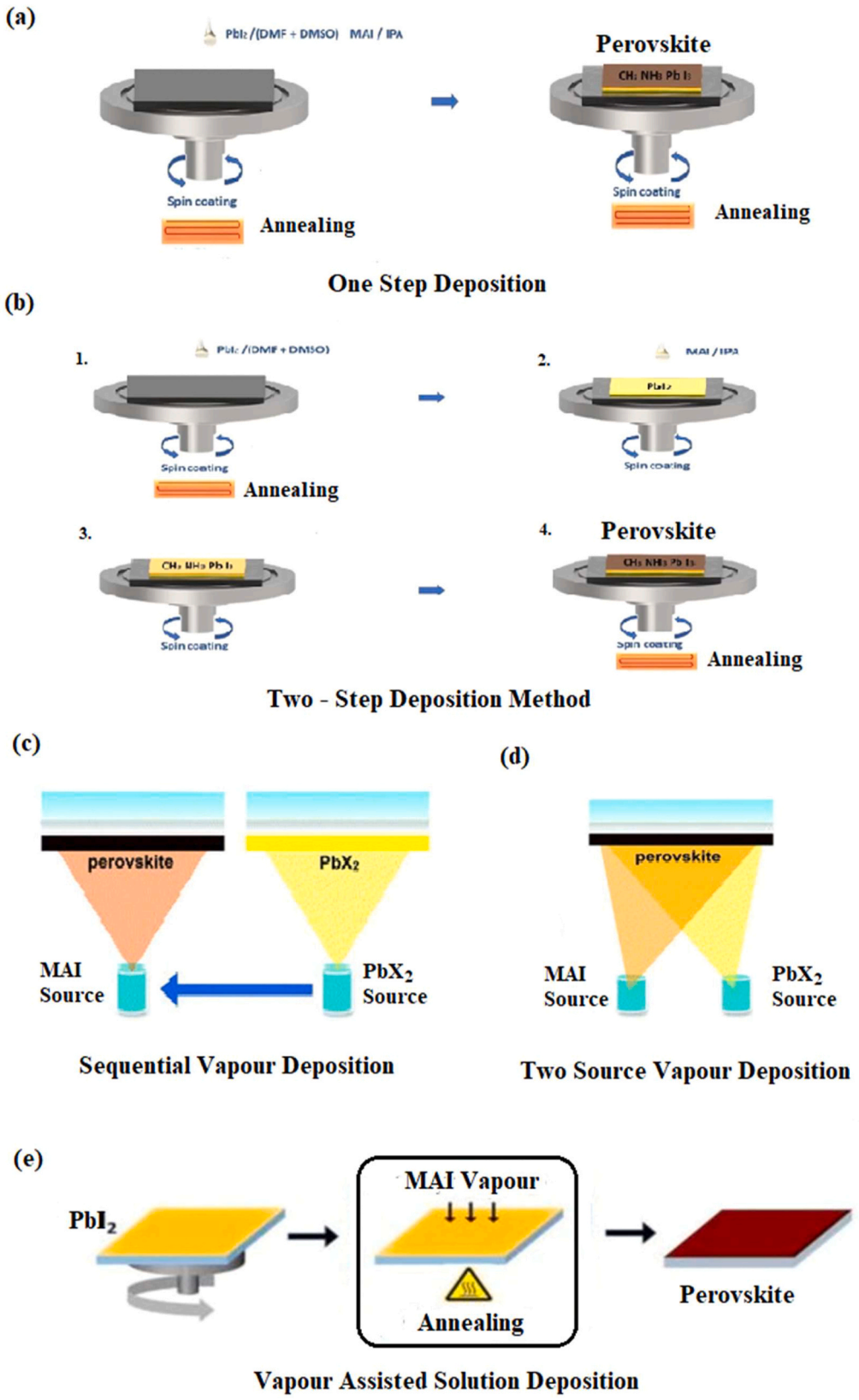

Fig. 6. Schematic illustration of most common fabrication methods of perovskite thin film.

ZrO_2/carbon device structure for the analysis of the factors responsible for causing the hysteresis effect. The study reveals that not only thickness, fabrication process, and pore size are the parameters that influence the hysteresis effect but also parameters such as accumulation of charges at the interfaces, recombination of charges, and ion migration are the important factors causing the hysteresis effect. The results showed the

presence of a barrier for ionic and electronic carriers at the interface of FTO/c-TiO_2/perovskite layers which causes charge accumulation at the surface of the layers by causing a recombination effect. However, in this approach, the recombination effect is rectified by employing mesoporous TiO_2 in between FTO and c-TiO_2 layer which facilitates better separation and transportation at the interfaces. A maximum PCE of 12.77% forward scan and 12.78% reverse scan were obtained for the reported device structure with a very low hysteresis effect index of 0.0010 ± 0.0035, V_{oc} of 0.91 V, J_{sc} of 21.40 mA/cm^2 and FF of 0.65 is estimated (Rong et al., 2017).

Kim *et al.* examined the influence of parameters causing the hysteresis effect in $CH_3NH_3PbI_3$-based perovskite solar cells. Variations were made in the thickness of the electron transport layer from 0 nm (planer structure), 110 nm, and 220 nm for the crystal size of perovskite 440 nm which were prepared using the sequential deposition method. All of the samples retained the same perovskite layer thickness. The results indicated a specific capacitance absorbed at the interfaces of ETL and the active layer due to slow charge separation and transportation. With a rise in the crystalline size of the perovskite, there was a drop in the capacitance at the interface of ETL/Perovskite by reducing the hysteresis effect. Also, introduces a mesoporous TiO_2 electron transport layer resulting in quick separation, transportation of charges, and suppression of the capacitance effect. Efficiency for the optimum thickness of the electron transport layer 220 nm and the crystalline size of the perovskite 440 nm is estimated to be 11.5% with a hysteresis index of 0.059. The efficiency for planner structure 0 nm was estimated to be 6.3% for the 0.362 hysteresis index (Kim and Park, 2014).

Ma *et al.* studied the impact of TiO_2/CdS ETL in their examination of the performance of $CH_3NH_3PbI_3$-based PSCs. The quantitative correlation was performed for TiO_2 and TiO_2/CdS-based perovskite solar cells fabricated using the microwave hydrothermal method at various time intervals of 10, 20, 30, 40, and 50 mins. The results showed the cell fabricated using TiO_2/CdS-30 mins, performed a greater PCE of 14.26% than the cell fabricated using TiO_2 with an efficiency of 10.3% (Ma et al., 2016). Varied power conversion efficiency was observed for the device fabricated at different time intervals due to uneven surface coverage of CdS above the TiO_2 layer. However, with an increase in the deposition time above 40 and 50 mins, there was a decrease in PCE due to the thicker CdS layer resulting in the transmittance of lesser light intensity to the perovskite layer. A decrease in charge accumulation and enhanced charge transportation at the interface of electron transport and perovskite layer was done by employing the CdS layer in between TiO_2 and perovskite layers (Habisreutinger et al., 2014).

According to the findings of Zhuowei Gu *et al.* a 10-minute UV-Ozone treatment on the surface of a CdS nanorod array for a perovskite solar cell resulted in an 8.36% enhancement in PCE (Gu et al., 2015). In contrast, Wei Liu *et al.* fabricated a PSC with TiO_2/CdS core – shell NAs by chemical bath deposition method and measured the highest PCE of 17.71% (Liu et al., 2019). Wiley A Dunlap-Shohl *et.al.*, on further lowering the particle size of CdS to 30 nm using the chemical bath deposition approach, 15% more PCE was recorded for $(CH_3NH_3)_2CdI_4$ based perovskite solar cells (Dunlap-shohl et al., 2016). NK Elangovan *et al.* have investigated the impact of a CdS-based ETL on perovskite solar cell performance. Chemical bath deposition was used to fabricate CdS at various time intervals of 10, 20, and 30 min. The results show that increasing the deposition time causes an increase in microstrain, dislocation density, and series resistance, all of which have a strong impact on the performance of the PSC (Sivaprakasam and Elangovan, 2021).

3.4. Band gap's influence on PSCs performance

It is critical to develop efficient electron and hole transport materials with appropriate energy levels to build highly efficient and stable PSCs. Perovskite's electrical and optical properties are greatly influenced by the band structure derived from the allowable quantum mechanical wave functions in the perovskite crystal. However, the band gap of the selected materials is more important for visible light absorption, reduction of capacitive effect at the interfacial layers, and maintaining device stability. Notably, the large band gap of ETL restricts light absorption and decreases photo generation. The matching band structure in PSC is also the primary cause of the rapid separation of electrons and holes, which quickly dissipates capacitive charges and reduces the hysteresis effect. Fig. 7 illustrates the perovskite structure ABX_3, device configuration, and energy band diagram of perovskite solar cells.

Band gap engineering, as a result, plays a significant part in realizing highly efficient PSCs. A standard anatase TiO_2 with a band gap of Eg = 3.2 eV can absorb just 5% of solar energy, which affects solar cell output and performance. Thus, researchers have explored doping metals (V, Fe, Cr, Ni) or non-metals (S, F, C, N, B) with TiO_2 to increase UV–visible light photocatalysis. Doping of both metals and non-metals along with TiO_2 improves the quality of semiconductor material by increasing the absorption range and increases the mobility of the charge carriers (Islam et al., 2017). The charge separation and transportation in PSCs are controlled by the energy band alignment and built-in internal electrical field. Ming Wang *et al.*, developed a perovskite solar cell with the device configuration ITO/PEDOT: PSS/$MAPbI_{3-X}Cl_X$/PCBM/Rhoda-mine101/LiF/Ag to investigate how band gap tuning in the perovskite layer leads in rapid hole extraction (Wang et al., 2018b). As the concentration of MAI increases, the material's band gap is reduced by increasing quick charge transportation, increasing current density. As a result, with an increasing MAI concentration of 4 mg/ml, the Jsc was increased to 23.52 mA/cm^2, resulting in a high PCE of 16.67% in the $MAPbI_{3-x}Cl_x$-based perovskite solar cells.

Zhang *et al.* examine the impact of tuning the band gap on performance in perovskite solar cells. Sb is incorporated into $CH_3NH_3PbI_3$ material to tune the band gap of perovskite material, and the band gap is regulated from 1.55 to 2.06 eV. A larger band gap results from reduced Pb bonding caused by stronger Sb interaction with $CH_3NH_3PbI_3$ material. Optimum doping of Sb content causes increasing electron density in the conduction band and raises the quasi-Fermi energy level (Zhang et al., 2016). As a result, the built-in potential in Sb-1% is increased, resulting in a significant increase in Voc and an advancement in electron transportation. The performance of the Sb-1% doped solar cell is better than the Sb-100% doped solar cell. Other than that, the *Jsc* of Sb-1% is increased due to the long charge diffusion length, which ensures efficient charge transport and collection. However, increased trap states, which degrade the Jsc, cause further reduction in Sb-100% doped devices.

Prasanna *et al.* have studied the effect of band gap tuning of perovskite material for solar photovoltaic applications. In PSCs, tin and lead iodide perovskite semiconductors are leading candidates, in part because their band gaps can be altered across a broad range through compositional modification. Due to octahedral tilting, lead iodide-based perovskites demonstrate an increase in band gap with partial replacement of formamidinium and cesium. Tin-based perovskites, on the other hand, exhibit the reverse tendency, with no octahedral tilting, resulting in a progressive reduction of the band gap. The band gaps created by this compositional tuning are nearly ideal for use of a tandem-based perovskite solar cell, capable of harvesting light out to around 1040 nm in the solar spectrum. According to the study, ideal perovskite solar cells require unique material properties, such as a direct and appropriate band gap, a sharp band edge, a long charge carrier lifespan, a long diffusion length, and a low exciton binding energy. Band gap engineering strategies are critical for optimizing energy band structures, which have a significant impact on light harvesting and PCE (Prasanna et al., 2017; Hu et al., 2019). Fig. 8 depicts the band gap and energy band alignment of various perovskite, electron, and hole transport materials (Kulkarni et al., 2014).

3.5. Stability

Compared to silicon solar cells, PSCs have stability difficulties

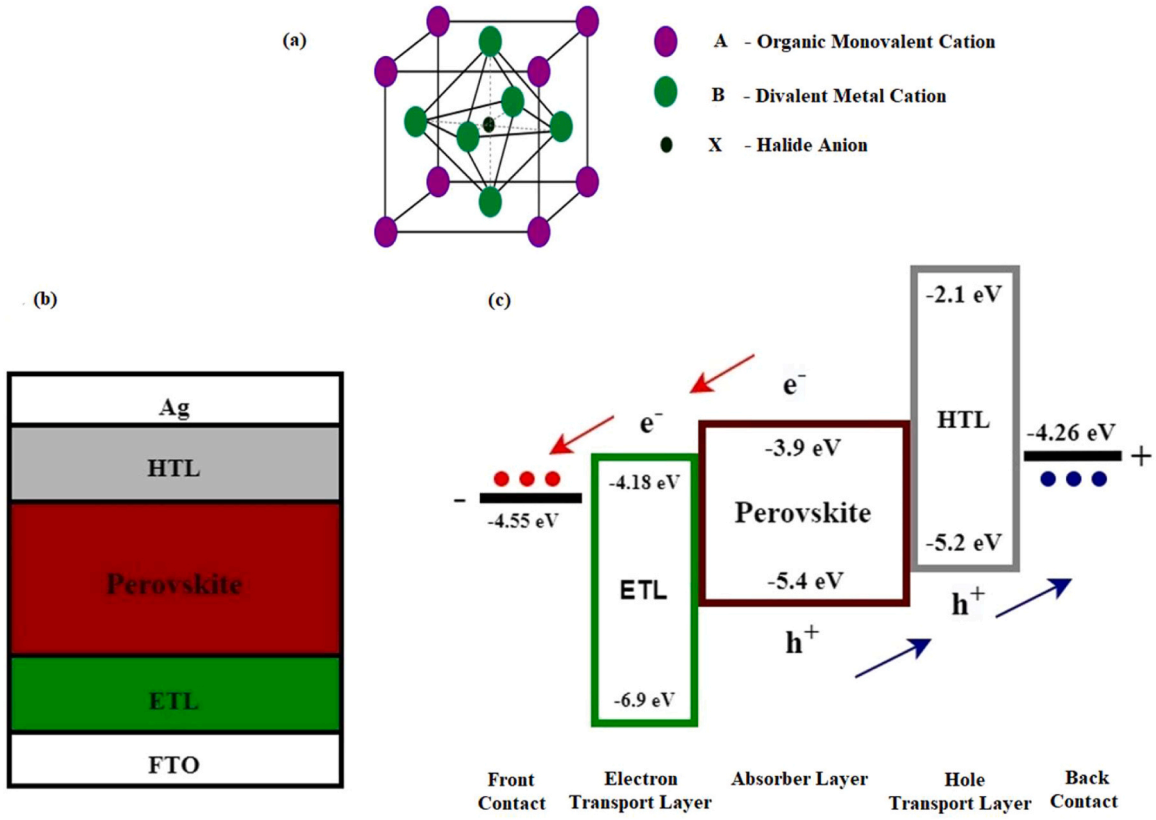

Fig. 7. (a) Schematic illustration of perovskite structure ABX_3 (b) Device configuration of PSC (c) Energy band diagram of PSC.

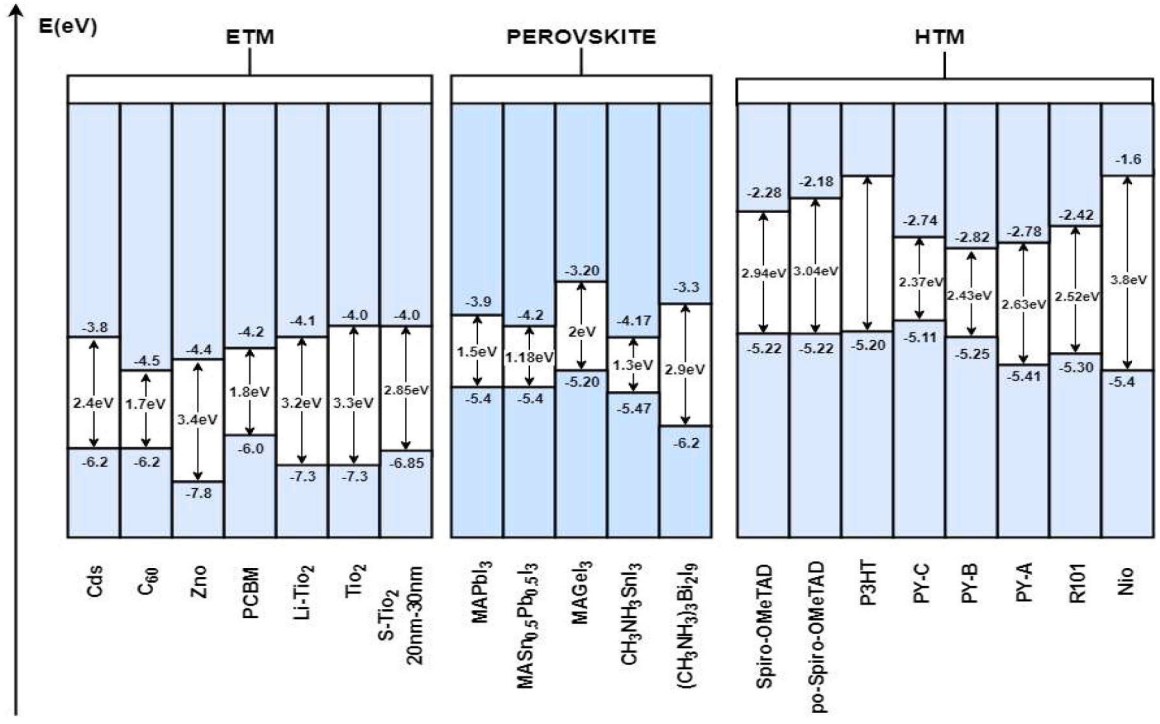

Fig. 8. Various ETM, HTM, and Perovskite energy band gap diagrams.

despite significant increases in high PCE and cheap production costs. Each type of device has different concerns about degradation mechanisms. For instance, depending on the characteristics of the solar cell, all types of solar cells require a special encapsulation because they are sensitive to moisture, oxygen, elevated temperature, and UV illumination to varying degrees. The device stability, degradation issues, and practical efficiency of a PSC, which is still under investigation, remain the most significant barriers to commercialization. Fig. 9 depicts a classification of various stability issues in PSCs. The origin of the intrinsic stability issue is due to phase instability in PSCs caused by the Perovskite crystal structure and PSC device configuration. Table 4 shows examples of various PSC device configurations with PCE and device stability, as well as the results of the respective stability test information.

An ideal perovskite has a cubic structure and ABX3 material combinations. A represents a higher monovalent cation, B is a smaller bivalent, and X is a monovalent anion. The Goldschmidt tolerance factor t can forecast a perovskite structure's stability. The stable perovskite crystal structure with a tolerance factor of 0.7 to 1.0 is preferable. Perovskite crystal structure lattice distortion can induce device instability if the tolerance factor exceeds the acceptable limit.

$$t = \frac{RA + RX}{\sqrt{2}(RX + RB)} \tag{1}$$

RA, RB, and RX denote the ionic radii of the A, B, and X ions. In an ideal case, $1 > t > 0.9$ yields a cubic structure, $t > 1$ yield tetragonal or hexagonal structures, $0.9 > t > 0.7$ yields rhombohedral or orthorhombic structure, and $t < 0.7$ yields no perovskite crystal structure. However, perovskite inevitably has internal defects, such as Pb and I vacancy defects, particularly near the gain border, which diminishes the stability and performance of PSC. Doping metal ions is currently an effective method for reducing defects, which can increase PSC stability and efficiency (Zhao et al., 2017; Gong et al., 2018). Furthermore, the performance of PSC was improved by doping with monovalent metal cations (Li^+, Cu^+, or Ag^+), which reduced trap-state density, enhanced perovskite crystallinity, and improved film quality (Zhang et al., 2019, 2017; Klug et al., 2016). To increase the stability of PSC, bivalent cations (Zn^{2+}, Mn^{2+}, or Co^{2+}) were doped. To reduce deep flaws, improve film shape, and boost the effectiveness and stability of PSC, trivalent metal cations (In^{3+}, Eu^{3+}, and Al^{3+}) were frequently utilized (Shi et al., 2017; Xu et al., 2018; Wang et al., 2016, 2019b; Lu et al., 2019; Xiao et al., 2019). With 92% of the original PCE under constant illumination for 1500 h, the device provides long-term endurance, particularly with Eu^{3+} doping (Wang et al., 2019c). The stability issues caused by band gap alignment were discussed in the previous section. Perovskites, on the other hand, when used in PSC devices are subject to external factors like environmental stability, thermal stability, and photo-stability, all of which have an impact on long-term stability. The most important factor contributing to environmental stability issues in PSCs is encapsulation. Encapsulation is an effective method for extending the life of solar cells and controlling degradation issues by acting as an oxygen and moisture barrier. For example, the dominant factors causing instability are H_2O, O_2, ultraviolet light and heat. When $MAPbI_3$-based perovskite is subjected to humid circumstances, hydrolysis reaction weakens hydrogen bonds in the crystal lattices, degrading PbI_2 and changing its colour from dark brown to yellow. Recent attempts have shown improvement in extrinsically increasing the device stability of perovskite solar cells by incorporating glass to glass encapsulation, hydrophobic coating, and substituting reactive metal electrodes with non-corrosive carbon or

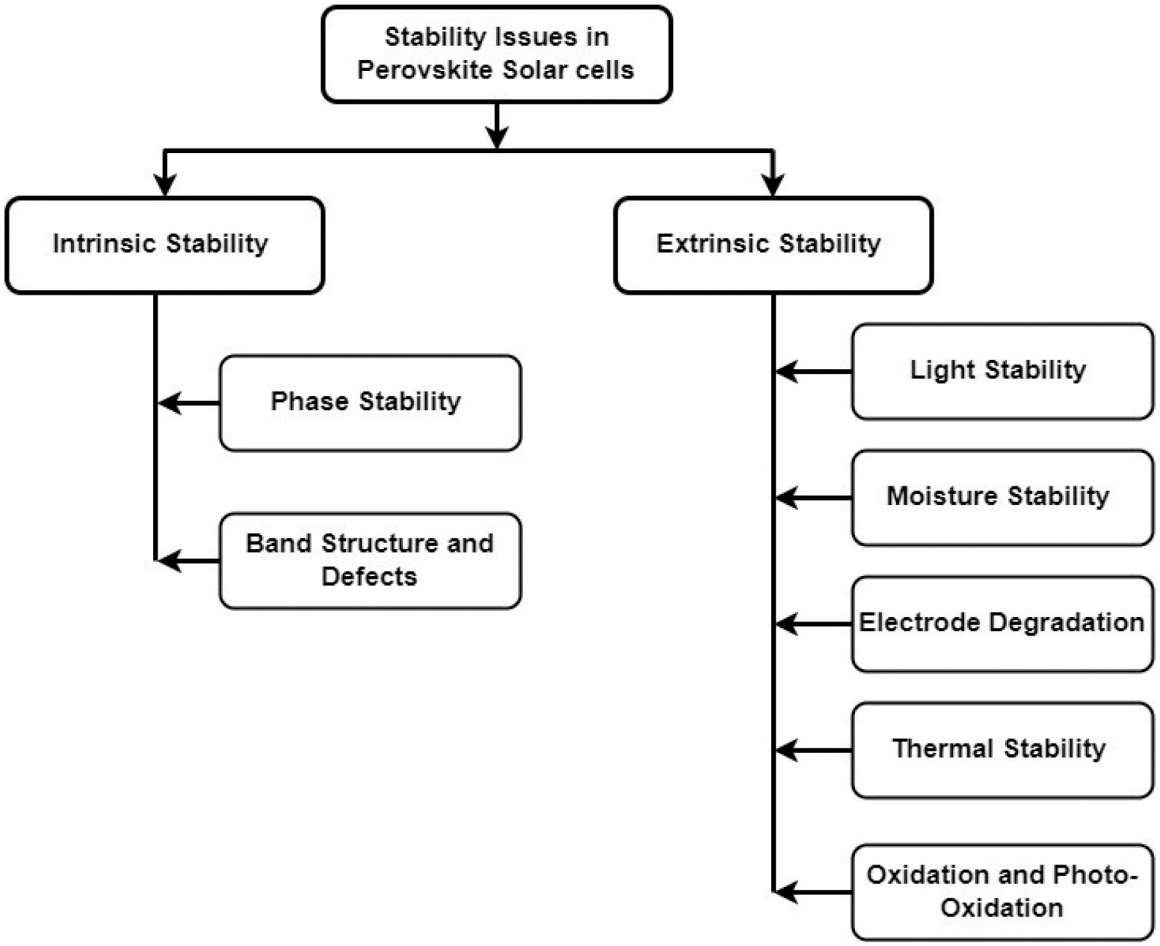

Fig. 9. Illustrates various stability issues in Perovskite solar cells.

Table 4
The impact of various PSC device configurations on stability and PCE.

SI. NO	Device Configuration	Stability	PCE	Year	Reference
1	ITO/HTL-Free/MAPbI3/C60/BCP/Ag	After 1000 h of light soaking at maximum power point tracking (MPPT), 93% of PCE was retained	16.9	2019	(Zhou et al., 2019)
2	FTO/NiMgLiO$_x$/FAMAPbI$_3$/PCBM/Ti(Nb)Ox/ Ag	After 500 h of continuous light soaking at MPPT, ambient conditions, and an encapsulated device, efficiency drops by 15%. After 500 h of thermal stress at 85 °C in the dark, the PCE drop was less than 10%.	20.6	2017	(Xie et al., 2017)
3	FTO/meso-TiO$_2$/CsFAMAPbI$_{3-x}$Brx/CuSCN-rGO/Au	PCE drop of 5% for more than 1000 h at MPPT, at 60 °C	20.2	2017	(Arora et al., 2017)
4	FTO/c-TiO$_2$/m-TiO$_2$/ (FAPbI$_3$)$_{0.95}$(MAPbBr$_3$)$_{0.05}$/ WBH/P3HT/Au	At MPPT, 25 °C, there is a 5% PCE drop for > 1370 h.	22.7	2019	(Jung et al., 2019)
5	FTO/Ru-doped SnO$_2$/perovskite/Spiro-OMeTAD(Zn- TFSI2)/Au	Over 2000 h, there was only a 3% decrease in efficiency (MPPT).	21.8	2019	(Akin, 2019)
6	FTO/TiO$_2$(Na-TFSI)/ (FAPbI$_3$)$_{0.95}$(MAPbBr$_3$)$_{0.05}$/Spiro- OMeTAD(Na-TFSI)/Au FTO/TiO$_2$	Na-TFSI has long-term operating stability at 45 °C, with > 80% of initial performance remaining even after 500 h.	22.4	2020	(Bang et al., 2020)
7	ITO/NiO$_x$/MAPbI$_3$/ZnO/Al	All metal oxide devices continue to maintain approximately 90% of their original efficiency after 60 days in air at room temperature.	16.1	2016	(You et al., 2016)
8	ITO/SnO$_2$/MAPbI$_3$/PTAA/Ag	Under continuous annealing at 85 °C in N$_2$, they continue to maintain more than 85% of their efficiency.	20.2	2019	(Wang et al., 2019a)
9	ITO/SnO$_2$/FA$_{0.95}$Cs$_{0.05}$PbI$_3$/Spiro-OMeTAD/Au	PSC degrades only 8% after 2880 h in an ambient atmosphere, and 14% after 120 h of irradiation at 100 mW cm^{-2}.	21.6	2018	(Yang et al., 2018)
10	FTO/compact-TiO$_2$/CdS//MAPbI$_3$/ Spiro-OMeTAD/Au	After 12 h of full sunlight illumination, CdS/PSC demonstrated significantly improved light stability, retaining nearly 80% of its initial efficiency.	9.9	2015	(Hwang et al., 2015)
11	ITO/P3CTN/(FAPbI$_3$)$_{0.95}$(MAPbBr$_3$)$_{0.05}$/ TMTAIBL/PCBM/C60/ TPBi/Cu	For 1000 h under continuous illumination at 60 °C, operational stability was 80% of initial efficiency at MPPT. They also have good thermal stability and retain more than 90% of their initial efficiency after 1000 h of aging at 60 °C.	19.2	2019	(Li et al., 2019)
12	FTO/mp-TiO$_2$/CdS:Cd(SCN$_2$H$_4$)$_2$Cl$_2$/ CH$_3$NH$_3$PbI$_3$/Spiro-OMeTAD/Au	After 240 h, PSCs without CdS: Cd(SCN$_2$H$_4$)$_2$Cl$_2$ retained 23.4% of the initial value, whereas with CdS and Cd(SCN$_2$H$_4$)$_2$Cl$_2$ retained 86.2% of the initial value.	20.1	2022	(Zheng et al., 2022)
13	FA$_{0.83}$Cs$_{0.17}$PbI$_3$/CuPc - HTL	The device showed exceptional long-term stability, maintaining its efficiency after over 5000 h in storage and 3700 h under 85 °C in a N$_2$ environment.	13.9	2023	(Snaith et al., 2023a)

transparent conducting oxides. These approaches directly protect perovskite devices from the ambient environment. For example, an electron beam-deposited SiO_2 layer inside a glass cover layer has good long-term stability. To improve long-term stability, various encapsulation materials are being explored, including ethylene methyl acrylate, ethylene vinyl acetate, polyisobutylene etc. The glass-polymer-glass structure, in general, prevents moisture ingress. The polymers and epoxy resin act as a glass adhesive and edge sealant.

Another factor is thermal stability. Thermal annealing at high temperatures can damage components or device design. When perovskite is heated above 100 °C, leads to the formation of more PbI_2 and organic salts, resulting in poor performance. Here, the replacement of TiO_2 with CdS as the electron transport layer and Spiro-OMeTAD with carbon nanotubes uniformly wrapped with a conductive polymer such as P3HT as the hole transport layer, would increase thermal stability and improve the surface morphology of the device. Moreover, the maximum stability of PSC has a lifetime of 4000 h of continuous light exposure at laboratory test conditions in which the efficiency decreases with an increase in degradation. Overall, encapsulation issues, and photo and thermal stability are the primary causes of stability issues in PSCs.

Also crucial is PSC photo stability. Photo bleaching effect and devices without encapsulation construction cause photo instability, especially for devices with TiO2, since the electron transport layer (sensitive to ultraviolet light) decomposes intrinsic material under UV irradiation. However, anti-UV coating on the FTO glass may eliminate the photo stability issue. Adding additional layers can sometimes improve long-term stability. In general, these interlayers should have high light transmission, improved electrical properties, and no reaction with other components. They typically suppress charge recombination, modify the surface of perovskite, prevent moisture ingress, and prevent the diffusion of other materials. As a result, the presence of these additional layers can improve perovskite solar cell stability. Experiments have shown that the lifetime of PSCs at 35 °C is about 0.7 years if 25% degradation is used as a standard. It is significantly less than the lifetime of crystalline silicon solar cells (Wang and Hou, 2021). Fig. 10 summarizes the factors that influence the performance of perovskite solar cells.

Henry J Snaith and his research team conducted a noteworthy investigation into inverted perovskite solar cells utilizing a hole transport layer composed of copper phthalocyanine (CuPc). This study revealed compelling findings, particularly in terms of long-term stability. The solar cell device exhibited remarkable resilience, retaining its efficiency even after undergoing extensive testing, including over 5000 h of storage and 3700 h of exposure to elevated temperatures at 85 °C in a nitrogen (N_2) environment (Snaith et al., 2023a, 2023b). The emphasis on the (CuPc) hole transport layer adds significance to the research, as the choice of materials in perovskite solar cells plays a pivotal role in determining their performance and stability. The extended storage and thermal exposure tests not only showcase the durability of the device but also suggest the potential practicality of these inverted perovskite solar cells in real-world applications. Furthermore, the results from this study contribute valuable insights to the broader understanding of perovskite solar cell technology. The exceptional long-term stability observed under various conditions is crucial information for researchers and engineers working on the development of solar energy technologies, offering a potential avenue for improving the reliability and lifespan of perovskite-based devices. Researchers at China's University of Electronic Science and Technology have achieved one of the highest reported enhanced stability levels for PSC to date by passivating defects at the grain boundary and greatly hindering recombination. They accomplished this by polymerizing and fluorinating a Lewis acid of 4,4-bis (4-hydroxyphenyl) pentanoic acid, resulting in a fluorinated oligomer (FO-19) that is synthesized and used to passivate these defects in methylammonium lead iodide ($MAPbI_3$). They demonstrated that the carboxyl bond of FO-19 in the perovskite crystals was coordinated with Pb ions, effectively passivating the perovskite film's defects. As a result, the PCE for the inverted $MAPbI_3$-based PSC reported by the FO-19 device was 21.23% and the humidity and thermal stability of the PSC was also improved. The perovskite/silicon tandem solar cell is a viable option that can overcome

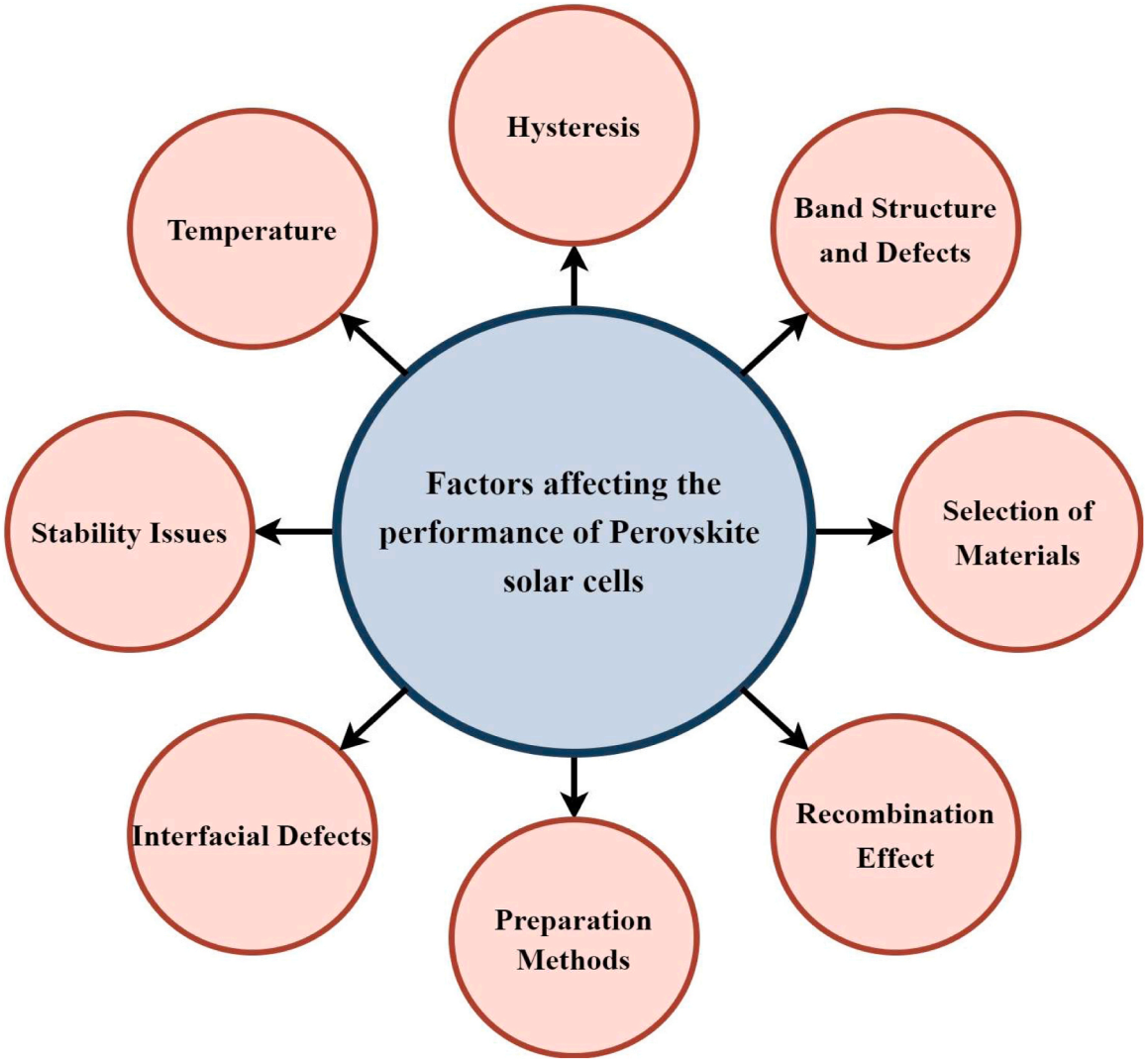

Fig. 10. Factors affecting the performance of perovskite solar cells.

efficiency limitations and stability. Using the evaporation-solution combination technique, Li *et al.* fabricated a p-i-n type perovskite on top of a fully textured silicon cell. The Perovskite/Si tandem cell has a 27.48% of PCE and is stable in nitrogen for 10,000 h (Li et al., 2021b). However, when compared to perovskite solar cells, the stability issue in silicon solar cells is much better, lasting nearly 30 years. This is due to the long-term developments in silicon solar cell technology over the last 50 years, which have resulted in silicon solar cells being highly stable, having an improved power conversion efficiency, and being commercially successful (Deng et al., 2006; Seal et al., 2013; Hofstetter et al., 2009; Lin et al., 2013; Mil et al., 2016; Narasimha and Rohatgi, 1998; Elangovan and Sivaprakasam, 2020; Voz et al., 2012; Islam and Ismail, 2013; Feifel et al., 2015; Nam et al., 2008). In just 10 years of research, perovskite solar cells have a high power conversion efficiency when compared to silicon solar cells. However, it is anticipated that stability issues with perovskite solar cells will be resolved in the future with the continuous study.

4. Innovations, key findings, and contributions

4.1. Innovations

The innovation of this article lies in its pursuit of advancing the controlled synthesis of perovskite heterojunctions—a critical aspect for both scientific exploration and practical applications. While the concept of constructing novel structural perovskite heterojunctions is straightforward, the article addresses the significant challenge of achieving controlled and predictable outcomes in practice. The research emphasizes the need for a comprehensive design principle to guide the synthesis of perovskite materials, moving beyond the trial-and-error approach. This is crucial for cultivating high-quality crystal structures devoid of defects and with regulated dimensionality. Furthermore, the article recognizes the infancy of hybrid perovskite research, emphasizing the necessity for fundamental studies to comprehensively understand their electrical, optical, and physical properties before practical applications, particularly in perovskite solar cells (PSCs). The exploration of alternative synthetic pathways to the commonly used solution process is highlighted, acknowledging the limitations and seeking innovative approaches.

A significant contribution comes from the exploration of morphologically low-dimensional structures, such as nanorods, nanocrystals, nanoplatelets, nanosheets, and nanowires, as a means to adjust the physical characteristics of perovskite materials. This adds a novel dimension to the synthetic strategies employed in perovskite research. Moreover, the study delves into the sensitized structure or tandem film structure of perovskite solar cells, introducing a wide range of materials for use as electron transport layers (ETL), hole transport layers (HTL), and active layers. Notably, the research highlights the need for

developing novel, low-cost hole transport materials to promote the commercialization of perovskite solar cells. This emphasis on cost-effective materials aligns with the practical considerations for scalability and widespread adoption of perovskite solar cell technology. Overall, the article's innovative approach and comprehensive exploration make significant strides in advancing the understanding and practical applications of perovskite materials.

4.2. Findings and contributions

The regulation of size, morphology, and structure in perovskite heterojunctions is essential for both scientific investigation and practical applications. The construction of novel structural perovskite heterojunctions is a relatively straightforward task conceptually, but achieving controlled and predictable outcomes in practise is a significant difficulty. In order to attain the objective of controlled synthesis, enhanced structural properties and achieving precious control over crystal formation remains a challenge. The extensive range of perovskite-based combinations presents a significant opportunity for exploration and investigation.

The synthesis of new perovskite materials continues to rely mostly on the trial and error approach. The development of a comprehensive design principle is important in order to cultivate high-quality crystal structures that are devoid of defects and possess regulated dimensionality. As hybrid perovskite research is still in its infancy, additional fundamental study is required to get a comprehensive understanding of their electrical, optical, and physical properties before PSCs utilised in real-world applications. The majority of perovskite material synthesis methods used today are based on the solution process, including anti solvent vapour assisted, hot injection, solvent diffusion, inverse temperature, temperature decreasing, and solvent evaporation crystallisation. Consequently, it is essential to develop alternative synthetic pathways to the solution process. Another efficient way to adjust the physical characteristics of the perovskite materials is to synthesise morphologically low dimensional structures such as nanorods, nanocrystals, nanoplatelets, nanosheets and nanowires (Bokdam et al., 2016; Protesescu et al., 2015; Herz, 2017; Dastidar et al., 2017; He et al., 2021; Min Nam et al., 2010).

The sensitized structure or tandem film structure of each of these perovskite solar cells involves the formation of heterojunctions between the perovskite material and a variety of other materials. In this study, a wide range of materials including SiO_2, TiO_2, CdS, ZnO, PEDOT:PSS, NiOx, Spiro-OMeTAD, PCBM, $MAPbI_3$, $MAPbBr_3$, $MASnI_3$, $CsPbBr_3$, $FASnI_3$ etc., have been developed for use as ETL, HTL, and active layers in PSCs (Acik and Darling, 2016; Batmunkh et al., 2017; Tong et al., 2017; Abulikemu et al., 2017; Mohamadkhani et al., 2019; Kim et al., 2020; Wang et al., 2021b; Patil et al., 2020; Ke et al., 2014; Liu and Kelly, 2014; Dong et al., 2014). Particularly Spiro-OMeTAD, the hole-transporting substance utilised in perovskite solar cells, is more costly and requires a complex synthesis process. To promote the commercialization of perovskite solar cells, it is necessary to develop novel, low-cost hole transport materials.

5. Recommendations and suggestions for future study

The surge in global research on perovskite can be attributed to their significant role in solar cells, which have seen substantial progress in performance over the last decade. In addition, the Pb element used in perovskite solar cells is extremely hazardous, which will inhibit the industrial promotion and development of PSCs. Therefore, a low-toxicity or nontoxic component must be found to take the place of Pb in the future. A comprehensive comprehension of the properties and mechanisms of materials allows the use of precisely delineated perovskite heterojunctions for many other applications.

5.1. Water splitting

A potential of 1.23 V is necessary for the process of water photolysis. In contrast, the substantial bandgap and considerable voltage shown by inorganic perovskite solar cells (PSCs) render them very suitable for the process of water photolysis. Perovskite-based photoelectrochemical cells have demonstrated a solar-driven water-splitting efficiency of 20.8% (Fehr et al., 2023). However, the limited duration of their water splitting capability hampers the progress of future research and development in this area. In prospective scenarios, the use of a hydrophobic coating holds promise for the purpose of segregating water and prolonging the lifespan of inorganic perovskite solar cells (PSCs).

5.2. Tandem perovskite/silicon solar cells

The achievement of a power conversion efficiency that exceeds the theoretical limit set by the Shockley-Queisser model for single-junction solar cells can be achieved through the use of a tandem device architecture incorporating both perovskite and silicon solar cells. Tandem structures are designed to increase the efficacy of solar energy harvesting through the clustering of two or more solar cells. One possible approach to accomplish this would be to fabricate a tandem solar cell by integrating perovskite and silicon components. The first perovskite/Si two-terminal tandem solar cell was reported in 2015 by Mailoa et al., demonstrating an overall efficiency of 14.3% (Cheng and Ding, 2021). A collaborative work on a perovskite/Si tandem (monolithic) 2-terminal structure was published in 2016 by Stanford University and Arizona State University. The aforementioned construction attained an efficiency of 23.6%, certified by National Renewable Energy Laboratory (NREL) (Mailoa et al., 2015). In a further advancement in the year 2018, Oxford PV effectively deployed tandem solar perovskites, namely the perovskite/Si tandem (monolithic) and 2 T tandem configurations with a maximum PCE of 27.3% (National Renewable Energy Laboratory, 2023). As a notable improvement, the efficiency of tandem perovskite/silicon solar cells developed by HZB researchers and certified by Fraunchofer Institute for Solar Energy Systems achieved a record of 29.15% (Al-Ashouriet al. 2020). Approved by the European Solar Test Installation (ESTI), LONGi, a Chinese company, unveiled at the Intersolar Europe 2023 exhibition in Munich, Germany, on 14 June 2023, a new conversion efficiency of 33.5% for silicon-perovskite tandem solar cells utilising commercial CZ silicon wafers (LONGI, 2023).

5.3. Integrated photovoltaic building

Typically, photovoltaic solar panels used for electricity generation are installed on the rooftops of buildings. Nevertheless, photovoltaic (PV) systems have the capability to be incorporated into building structures and are progressively being utilised in novel manners throughout the building process of construction. The implementation of integrated photovoltaic building (IPB) encompasses the use of panels that are either installed on or incorporated into the outside walls, skylights, windows, and facades of the building (Mailoa et al., 2015; National Renewable Energy Laboratory, 2023; LONGI, 2023; De Bastiani et al., 2017; Wheeler et al., 2017; Shao et al., 2023; Chen et al., 2023; Shen et al., 2023). As a result, the IPB requirements differ from those of rooftop-mounted systems. PSC is an attractive material for IPB applications due to its improved optical properties, such as transparency and colour, in addition to its advantageous weight and shape. In addition, these materials possess photovoltaic and thermochromic characteristics that can be incorporated into energy-efficient structures to enable reversible pigment changes in response to variations in temperature (Cao et al., 2023). M. De Bastiani et al. synthesised perovskite inks from $MAPb(I_{1-X}Br_x)_3$ with variable x. An investigation revealed that the ink exhibited a yellow hue at lower temperatures but underwent a colour change: from orange at 60 °C to 90 °C, and from brilliant red to black at 120 °C (De Bastiani et al., 2017). Wheeler et al. reported on the

thermochromic layer made of a halide perovskite with various concentrations of methylamine ($MAPbI_{3\bullet x}CH_3NH_2$). In its coloured form, the PSC had 11.3% PCE for solar photothermal heating. The cell after cooling has an average efficiency of 16.3% (Wheeler et al., 2017).

6. Conclusion and outlook

In recent years, the performance of PSCs has improved significantly, and they are now regarded as an excellent replacement for silicon solar cells. We have outlined several methods for enhancing the performance of perovskite solar cells in this study, including the use of various fabrication techniques, the development of novel perovskite and charge transport materials, recent advancements in band gap engineering, and stability issues. Despite extensive research into the advancement of PSCs, major challenges remain. The majority of perovskite material synthesis methods used today are based on the solution process, including anti-solvent vapour assisted, hot injection, solvent diffusion, inverse temperature, temperature decreasing, and solvent evaporation crystallization. Consequently, it is essential to develop alternative synthetic pathways to the solution process. Another efficient way to adjust the physical characteristics of perovskite materials is to synthesize morphologically low dimensional structures such as nanorods, nanocrystals, nanoplatelets, nanosheets, and nanowires. As hybrid perovskite research is still in its infancy, an additional fundamental study is required to get a comprehensive understanding of their electrical, optical, and physical properties before PSCs are utilized in real-world applications.

The external environmental elements including humidity, temperature, and UV radiation have a significant impact on the stability of the organic lead halide perovskite, which results in low device stability. Therefore, to increase the viability of such devices, it will be crucial to create a high-stability device composition that includes the perovskite layer, charge transport layer, and electrode materials, as well as a simple and effective device fabrication technique. A wide range of materials, including SiO_2, TiO_2, CdS, ZnO, PEDOT: PSS, NiOx, Spiro-OMeTAD, PCBM, $MAPbI_3$, $MAPbBr_3$, $MASnI_3$, $CsPbBr_3$, $FASnI_3$, etc., have been developed for use as ETL, HTL, and active layers in PSCs to achieve high PCE and stability. Particularly Spiro-OMeTAD, the hole-transporting substance utilized in perovskite solar cells, is more costly and requires a complex synthesis process. To promote the commercialization of perovskite solar cells, it is necessary to develop novel, low-cost hole transport materials. In addition, the Pb element used in perovskite solar cells is extremely hazardous, which will inhibit the industrial promotion and development of PSCs. Therefore, a low-toxicity or nontoxic component must be found to take the place of Pb in the future. According to the study, all of the aforementioned problems significantly affect photogeneration, charge transportation, and stability in PV devices. To overcome these challenges, researchers are working on next-generation PSCs with improved PCE and long-term stability. As a result of systematic collaboration from a variety of scientific, engineering, and entrepreneurial communities, perovskite has the potential to outperform other PV technologies in the future.

Funding statement

This research was supported by Basic Science Research Program through the National Research Foundation of Korea (NRF) funded by the Ministry of Education (2020R1A2C1004743).

CRediT authorship contribution statement

Alsharif Mohammed H.: Data curation, Software. **Kim Mun-Kyeom:** Conceptualization, Funding acquisition, Writing – review & editing. **Inamul Hasan:** Investigation, Visualization. **Elangovan Naveen Kumar:** Formal analysis, Methodology, Writing – original draft. **Kannadasan Raju:** Resources, Writing – review & editing. **Beenarani B. B.:** Data curation, Validation.

Declaration of Competing Interest

The authors declare that they have no known competing financial interests or personal relationships that could have appeared to influence the work reported in this paper.

Data Availability

Data will be made available on request.

References

M. Abulikemu, J. Barbé, A. El, J. Eid, and S. Del, Planar heterojunction perovskite solar cell based on CdS electron transport layer, vol. 636, pp. 512–518, 2017.
Acik, M., Darling, S.B., 2016. Graphene in perovskite solar cells: device design, characterization and implementation. J. Mater. Chem. A vol. 4 (17), 6185–6235. https://doi.org/10.1039/c5ta09911k.
Akin, S., 2019. Hysteresis-free planar perovskite solar cells with a breakthrough efficiency of 22% and superior operational stability over 2000h. ACS Appl. Mater. Interfaces vol. 11 (43), 39998–40005. https://doi.org/10.1021/acsami.9b13876.
A. Al-Ashouri *et al.*, Monolithic perovskite/silicon tandem solar cell with >29% efficiency by enhanced hole extraction, Science (80–.)., vol. 370, no. 6522, pp. 1300–1309, 2020, doi: 10.1126/science.abd4016.
N. Arora *et al.*, Perovskite solar cells with CuSCN hole extraction layers yield stabilized efficiencies greater than 20%, Science (80–.)., vol. 358, no. 6364, pp. 768–771, 2017, doi: 10.1126/science.aam5655.
Bahtiar, A., Rahmanita, S., Inayatie, Y.D., 2017. Pin-hole free perovskite film for solar cells application prepared by controlled two-step spin-coating method. IOP Conf. Ser. Mater. Sci. Eng. vol. 196 (1) https://doi.org/10.1088/1757-899X/196/1/012037.
Bang, S.M., et al., 2020. Defect-tolerant sodium-based dopant in charge transport layers for highly efficient and stable perovskite solar cells. ACS Energy Lett. vol. 5 (4), 1198–1205. https://doi.org/10.1021/acsenergylett.0c00514.
Bati, A.S.R., Zhong, Y.L., Burn, P.L., et al., 2023. Next-generation applications for integrated perovskite solar cells. Commun. Mater. 4, 2 https://doi.org/10.1038/s43246-022-00325-4.
M. Batmunkh, C.J. Shearer, M. Bat-erdene, M.J. Biggs, and J.G. Shapter, Single-Walled Carbon Nanotubes Enhance the E ffi ciency and Stability of Mesoscopic Perovskite Solar Cells, 2017, doi: 10.1021/acsami.7b04894.
Bokdam, M., et al., 2016. Role of polar phonons in the photo excited state of metal halide perovskites. Sci. Rep. vol. 6 (i), 1–5. https://doi.org/10.1038/srep28618.
Cao, Yingjie, Wang, Yanan, Zhang, Yufeng, Liu, Xiaolin, Lin, Jia, 2023. Stable and rapid thermochromic reversibility in acene alkylamine intercalated layered hybrid perovskites. Mater. Today Commun. 107544, 2352–4928. https://doi.org/10.1016/j.mtcomm.2023.107544.
Chen, D., et al., 2019b. Enhancing material quality and device performance of perovskite solar cells via a facile regrowth way assisted by the DMF/Chlorobenzene mixed solution. Org. Electron. vol. 70 (February), 300–305. https://doi.org/10.1016/j.orgel.2019.04.012.
M. Chen *et al.*, Highly stable and ef fi cient all-inorganic lead-free perovskite solar cells with native-oxide passivation, no. 2019a, pp. 1–8, doi: 10.1038/s41467–018-07951-y.
Chen, P.-Y., Yang, S.-H., 2016. Improved efficiency of perovskite solar cells based on Ni-doped ZnO nanorod arrays and Li salt-doped P3HT layer for charge collection. Opt. Mater. Express vol. 6 (11), 3651. https://doi.org/10.1364/ome.6.003651.
Chen, Y., Zhou, Qi, Song, Huanping, Luo, Tze-Bin, Hong, Song, Duan, Ziruo, Dou, Hsin-Sheng, Liu, Letian, Yang, Yongsheng, 2014. Controllable self-induced passivation of hybrid lead iodide perovskites toward high performance solar cells. Am. Chem. Soc. vol. 14 (7) https://doi.org/10.1021/nl501838y.
Chen, Ying, Zhang, Man, Li, Fuqiang, Yang, Zhenyuan, 2023. Recent progress in perovskite solar cells: status and future. Coatings 13 (3), 644. https://doi.org/10.3390/coatings13030644.
Chen, Z., Zhang, H., Yao, F., Tao, C., Fang, G., Li, G., 2020. Room temperature formation of semiconductor Grade α-FAPbI3 films for efficient perovskite solar cells. Cell Rep. Phys. Sci. vol. 1 (9), 100205 https://doi.org/10.1016/j.xcrp.2020.100205.
Cheng, Y., Ding, L., 2021. Perovskite/Si tandem solar cells: fundamentals, advances, challenges, and novel applications. Sus. Mat. 1, 324–344.
Christians, J.A., Fung, R.C.M., Kamat, P.V., 2014. An inorganic hole conductor for organo-lead halide perovskite solar cells. improved hole conductivity with copper iodide. J. Am. Chem. Soc. vol. 136 (2), 758–764. https://doi.org/10.1021/ja411014k.
Dastidar, S., Li, S., Smolin, S.Y., Baxter, J.B., Fafarman, A.T., 2017. Slow electron-hole recombination in lead iodide perovskites does not require a molecular dipole. ACS Energy Lett. vol. 2 (10), 2239–2244. https://doi.org/10.1021/acsenergylett.7b00606.
De Bastiani, M., et al., 2017. Thermochromic perovskite inks for reversible smart window applications. Chem. Mater. 29, 3367–3370, 92.
Deng, X., et al., 2006. Fabrication and characterization of triple-junction amorphous silicon based solar cell with nanocrystalline silicon bottom cell. IEEE 4th World Conf.

Photovolt. Energy Conf. 1461–1464. https://doi.org/10.1109/WCPEC.2006.279744.
Dong, J., et al., 2014. Impressive enhancement in the cell performance of ZnO nanorod-based perovskite solar cells with Al-doped ZnO interfacial modification. Chem. Commun. vol. 50 (87), 13381–13384. https://doi.org/10.1039/c4cc04908j.
W.A. Dunlap-shohl, R. Younts, B. Gautam, K. Gundogdu, and D.B. Mitzi, Effects of Cd Diffusion and Doping in High-Performance Perovskite Solar Cells Using CdS as Electron Transport Layer, 2016, doi: 10.1021/acs.jpcc.6b05406.
Elangovan, N.K., Arumugam, S., . 2019. Chayaver: Indian-traditional dye to modern dye-sensitized solar cells. Mater. Res. Express vol. 6 (6), 066206. https://doi.org/10.1088/2053-1591/ab0cad.
Elangovan, N.K., Sivaprakasam, A., 2020. Investigation of parameters affecting the performance of Perovskite solar cells. Mol. Cryst. Liq. Cryst. vol. 710 (1), 66–73. https://doi.org/10.1080/15421406.2020.1829425.
Elumalai, N.K., Mahmud, M.A., Wang, D., Uddin, A., 2016. Perovskite solar cells: progress and advancements. Energies vol. 9 (11). https://doi.org/10.3390/en9110861.
European Commission. Restriction of Hazardous Substances in Electrical and Electronic Equipment (RoHS), (https://environment.ec.europa.eu/system/ files/2021-01/FAQ%20key%20guidance%20document%20-%20RoHS.pdf).
Fehr, A.M.K., et al., 2023. Integrated halide perovskite photoelectrochemical cells with solar-driven, 12 (1). https://doi.org/10.1038/s41467-023-39290-y.
M. Feifel *et al.*, Gallium Phosphide Window Layer for Silicon Solar Cells, pp. 1–7, 2015.
X. Gong *et al.*, Highly Efficient Perovskite Solar Cells via Nickel Passivation, vol. 1804286, pp. 1–8, 2018, doi: 10.1002/adfm.201804286.
Green, M.A., Dunlop, E.D., Levi, D.H., Hohl-Ebinger, J., Yoshita, M., Ho-Baillie, A.W.Y., 2019. Solar cell efficiency tables (version 54). Prog. Photovolt. Res. Appl. vol. 27 (7), 565–575. https://doi.org/10.1002/pip.3171.
Gu, Z., et al., 2015. Novel planar heterostructure perovskite solar cells with CdS nanorods array as electron transport layer. Sol. Energy Mater. Sol. Cells vol. 140, 396–404. https://doi.org/10.1016/j.solmat.2015.04.015.
Habisreutinger, S.N., Leijtens, T., Eperon, G.E., Stranks, S.D., Nicholas, R.J., Snaith, H.J., 2014. Enhanced hole extraction in perovskite solar cells through carbon nanotubes. J. Phys. Chem. Lett. vol. 5 (23), 4207–4212. https://doi.org/10.1021/jz5021795.
Hao, F., Stoumpos, C.C., Cao, D.H., Chang, R.P.H., Kanatzidis, M.G., 2014. Lead-free solid-state organic-inorganic halide perovskite solar cells. Nat. Photonics vol. 8 (6), 489–494. https://doi.org/10.1038/nphoton.2014.82.
Hasan, Z.I., Joshi, S., 2022. Halide-based CH 3 NH 3 PbI 3 hybrid perovskite thin films structural studies using synchrotron source X-ray diffraction. J. Mater. Sci. Mater. Electron. vol. 33 (20), 16369–16382. https://doi.org/10.1007/s10854-022-08528-8.
Hasan, Z.I., Joshi, S., Subbaya, K.M., Parameshwara, S., 2022. Surface interface structural studies of CH 3 NH 3 PbI 3 thin films using synchrotron source X-ray diffraction for solar cell application. Mater. Today Proc. vol. 64, 1837–1843. https://doi.org/10.1016/j.matpr.2022.06.185.
He, Y., et al., 2021. Demonstration of energy-resolved γ-ray detection at room temperature by the CsPBCl3 perovskite semiconductor. J. Am. Chem. Soc. vol. 143 (4), 2068–2077. https://doi.org/10.1021/jacs.0c12254.
Herz, L.M., 2017. Charge-carrier mobilities in metal halide perovskites: fundamental mechanisms and limits. ACS Energy Lett. vol. 2 (7), 1539–1548. https://doi.org/10.1021/acsenergylett.7b00276.
Hofstetter, J., Ca, C., Luque, A., 2009. Improvement of multi-crystalline silicon wafer quality during solar cell fabrication process. Span. Conf. Electron Devices 4–7. https://doi.org/10.1109/SCED.2009.4800510.
Hong, D., Xie, M., Tian, Y., 2021. Photostable and uniform ch3nh3pbi3 perovskite film prepared via stoichiometric modification and solvent engineering. Nanomaterials vol. 11 (2), 1–12. https://doi.org/10.3390/nano11020405.
Hu, Z., Lin, Z., Su, J., Zhang, J., Chang, J., Hao, Y., 2019. A review on energy band-gap engineering for perovskite photovoltaics. Sol. RRL vol. 3 (12), 1–9. https://doi.org/10.1002/solr.201900304.
Huang, Y.T., Kavanagh, S.R., Scanlon, D.O., Walsh, A., Hoye, R.L.Z., 2021. Perovskite-inspired materials for photovoltaics and beyond-from design to devices. Nanotechnology vol. 32 (13). https://doi.org/10.1088/1361-6528/abcf6d.
Hwang, I., Baek, M., Yong, K., 2015. Core/Shell structured TiO2/CdS electrode to enhance the light stability of perovskite solar cells. ACS Appl. Mater. Interfaces vol. 7 (50), 27863–27870. https://doi.org/10.1021/acsami.5b09442.
A.T.M.S. Islam and A.B. Ismail, Fabrication of uniform-macroporous silicon and its possible application in hybrid solar cell, pp. 401–404, 2013.
Islam, S.Z., Nagpure, S., Kim, D.Y., Rankin, S.E., 2017. Synthesis and catalytic applications of non-metal doped mesoporous titania. Inorganics vol. 5 (1). https://doi.org/10.3390/inorganics5010015.
Jeon, N.J., et al., 2014. O-methoxy substituents in spiro-OMeTAD for efficient inorganic-organic hybrid perovskite solar cells. J. Am. Chem. Soc. vol. 136 (22), 7837–7840. https://doi.org/10.1021/ja502824c.
Jeon, N.J., Lee, J., Noh, J.H., Nazeeruddin, M.K., Grätzel, M., Seok, S.Il, 2013. Efficient inorganic-organic hybrid perovskite solar cells based on pyrene arylamine derivatives as hole-transporting materials. J. Am. Chem. Soc. vol. 135 (51), 19087–19090. https://doi.org/10.1021/ja410659k.
Jiang, T., et al., 2019. Power conversion efficiency enhancement of low-bandgap mixed pb–sn perovskite solar cells by improved interfacial charge transfer. ACS Energy Lett. vol. 4 (7), 1784–1790. https://doi.org/10.1021/acsenergylett.9b00880.
Johansson, M.B., Johansson, E.M.J., Zhu, H., 2016. Extended photo-conversion spectrum in low- toxic bismuth halide perovskite solar cells. J. Phys. Chem. Lett. https://doi.org/10.1021/acs.jpclett.6b01452.
Joshi, S., Hasan, Z.I., Pruthvi, M., Tulsiram, M.P., 2021. A simplistic approach for perovskite based solar cells degradation studies. Mater. Today Proc. vol. 35, 31–34. https://doi.org/10.1016/j.matpr.2019.05.390.
Jung, E.H., et al., 2019. Efficient, stable and scalable perovskite solar cells using poly(3-hexylthiophene). Nature vol. 567 (7749), 511–515. https://doi.org/10.1038/s41586-019-1036-3.
KAUST Claims 33.7% Efficiency for Perovskite/Silicon Tandem Solar Cell. PV Magazine. 30 May 2023. Available online: https://www.pv-magazine.com/2023/05/30/kaust-claims-33–7-efficiency-for-perovskite-silicon-tandem-solar-cell/ (accessed on 12 July 2023).
Ke, W., et al., 2014. Perovskite solar cell with an efficient TiO2 compact film. ACS Appl. Mater. Interfaces vol. 6 (18), 15959–15965. https://doi.org/10.1021/am503728d.
Kim, H.S., Park, N.G., 2014. Parameters affecting I-V hysteresis of CH3NH3PbI3 perovskite solar cells: effects of perovskite crystal size and mesoporous TiO2 layer. J. Phys. Chem. Lett. vol. 5 (17), 2927–2934. https://doi.org/10.1021/jz501392m.
Kim, J., Kim, K.S., Myung, C.W., 2020. Efficient electron extraction of SnO2 electron transport layer for lead halide perovskite solar cell. npj Comput. Mater. vol. 6 (1), 1–8. https://doi.org/10.1038/s41524-020-00370-y.
M.T. Klug *et al.*, Environmental Science Tailoring metal halide perovskites through metal substitution: influence on photovoltaic and material properties †, 2016, doi: 10.1039/C6EE03201J.
Kojima, A., Teshima, K., Shirai, Y., Miyasaka, T., 2009. Organometal halide perovskites as visible-light sensitizers for photovoltaic cells. J. Am. Chem. Soc. vol. 131 (17), 6050–6051. https://doi.org/10.1021/ja809598r.
Krishnamoorthy, T., et al., 2015. Lead-free germanium iodide perovskite materials for photovoltaic applications. J. Mater. Chem. A vol. 3 (47), 23829–23832. https://doi.org/10.1039/c5ta05741h.
Krishnan, U., 2019. Factors affecting the stability of perovskite solar cells: a comprehensive review. J. Photonics Energy vol. 9 (02), 1. https://doi.org/10.1117/1.jpe.9.021001.
Kulkarni, S.A., Baikie, T., Boix, P.P., Yantara, N., Mathews, N., Mhaisalkar, S., 2014. Band-gap tuning of lead halide perovskites using a sequential deposition process. J. Mater. Chem. A vol. 2 (24), 9221–9225. https://doi.org/10.1039/c4ta00435c.
E.N. Kumar and S. Arumugam, Investigation of parameters affecting the performance of Perovskite solar cells, Mol. Cryst. Liq. Cryst., vol. 0, no. 0, pp. 1–8, doi: 10.1080/15421406.2020.1829425.
Lee, M.M., Teuscher, J., Miyasaka, T., Murakami, T.N., Snaith, H.J., 2012. Efficient hybrid solar cells based on meso-superstructured organometal halide perovskites. Science vol. 338 (6107), 643–647. https://doi.org/10.1126/science.1228604 ([doi]).
Lee, S.J., et al., 2016. Fabrication of efficient formamidinium tin iodide perovskite solar cells through SnF2-pyrazine complex. J. Am. Chem. Soc. vol. 138 (12), 3974–3977. https://doi.org/10.1021/jacs.6b00142.
Lekesi, L.P., Koao, L.F., Motloung, S.V., Motaung, T.E., Malevu, T., 2022. Developments on perovskite solar cells (PSCs): a critical review. Appl. Sci. vol. 12 (2) https://doi.org/10.3390/app12020672.
Li, H., et al., 2021a. Photoferroelectric perovskite solar cells: principles, advances and insights. Nano Today vol. 37, 101062. https://doi.org/10.1016/j.nantod.2020.101062.
Li, H., Fu, K., Hagfeldt, A., Grätzel, M., Mhaisalkar, S.G., Grimsdale, A.C., 2014. A simple 3,4-ethylenedioxythiophene based hole-transporting material for perovskite solar cells. Angew. Chem. - Int. Ed. vol. 53 (16), 4085–4088. https://doi.org/10.1002/anie.201310877.
X. Li *et al.*, E ffi cient Perovskite Solar Cells Depending on TiO 2 Nanorod Arrays, 2016b, doi: 10.1021/acsami.6b05971.
Li, X., et al., 2016c. A vacuum flash-assisted solution process for high-efficiency large-area perovskite solar cells. Sci, *Sci* vol. 1 (353(6294)), 58–62. https://doi.org/10.1126/science.aaf8060.
Li, X., et al., 2019. Suppressing the ions-induced degradation for operationally stable perovskite solar cells. Nano Energy vol. 64, 103962. https://doi.org/10.1016/j.nanoen.2019.103962.
Li, Y., et al., 2016a. 50% Sn-based planar perovskite solar cell with power conversion efficiency up to 13.6%. Adv. Energy Mater. vol. 6 (24), 1–7. https://doi.org/10.1002/aenm.201601353.
Li, Y., et al., 2021b. Wide bandgap interface layer induced stabilized perovskite/silicon tandem solar cells with stability over ten thousand hours. Adv. Energy Mater. vol. 11 (48), 1–9. https://doi.org/10.1002/aenm.202102046.
Lin, L., Jiang, L., Qiu, Y., Yu, Y., 2017. Modeling and analysis of HTM-free perovskite solar cells based on ZnO electron transport layer. Superlattices Micro vol. 104, 167–177. https://doi.org/10.1016/j.spmi.2017.02.028.
Lin, Y., Van Kerschaver, E., Cabanas-holmen, K., Solar, H., Llc, A., Clara, S., 2013. Laser sintering of screen-printed silver paste for silicon solar cells. IEEE 39th Photovolt. Spec. Conf. 3445–3447. https://doi.org/10.1109/PVSC.2013.6745189.
Liu, D., Kelly, T.L., 2014. Perovskite solar cells with a planar heterojunction structure prepared using room-temperature solution processing techniques. Nat. Photonics vol. 8 (2), 133–138. https://doi.org/10.1038/nphoton.2013.342.
Liu, D., Gangishetty, M.K., Kelly, T.L., 2014. Effect of CH3NH3PbI3 thickness on device efficiency in planar heterojunction perovskite solar cells. J. Mater. Chem. A vol. 2 (46), 19873–19881. https://doi.org/10.1039/c4ta02637c.
Liu, D., Shao, Z., Li, C., Pang, S., Yan, Y., Cui, G., 2021. Structural properties and stability of inorganic CsPbI 3 perovskites. Small Struct. vol. 2 (3), 2000089 https://doi.org/10.1002/sstr.202000089.
Liu, W., et al., 2019. Simultaneously enhanced efficiency and stability of perovskite solar cells with TiO 2 @CdS core–shell nanorods electron transport layer. Adv. Mater. Interfaces vol. 6 (5), 1–8. https://doi.org/10.1002/admi.201801976.

Liu, W., et al., 2020. Perfection of perovskite grain boundary passivation by rhodium incorporation for efficient and stable solar cells. Nano-Micro Lett. vol. 12 (1), 1–11. https://doi.org/10.1007/s40820-020-00457-7.
LONGI. 2023. Available online: https://www.longi.com/en/news/new-conversion-efficiency/ (accessed on 12 July 2023).
J. Lu, S. Chen, and Q. Zheng, Defect passivation of CsPbI 2 Br perovskites through Zn (II) doping: toward efficient and stable solar cells, vol. 62, no. 8, pp. 1044–1050, 2019.
Ma, Y., et al., 2016. Boosting efficiency and stability of perovskite solar cells with CdS Inserted at TiO2/Perovskite interface. Adv. Mater. Interfaces vol. 3 (22). https://doi.org/10.1002/admi.201600729.
Mailoa, J.P., Bailie, C.D., Johlin, E.C., Hoke, E.T., Akey, A.J., Nguyen, W.H., McGehee, M.D., Buonassisi, T., 2015. A 2-terminal perovskite/silicon multijunction solar cell enabled by a silicon tunnel junction. Appl. Phys. Lett. 106, 121105.
Mariyappan, P., Chowdhury, T.H., Subashchandran, S., Bedja, I., Ghaithan, H.M., Islam, A., 2020. Fabrication of Lead-free CsBi3I10 based compact perovskite thin films by employing solvent engineering and anti-solvent treatment techniques: an efficient photo-conversion efficiency up to 740nm. Sustain. Energy Fuels vol. 4 (10), 5042–5049. https://doi.org/10.1039/D0SE00786B.
McGovern, L., Futscher, M.H., Muscarella, L.A., Ehrler, B., 2020. Understanding the stability of MAPbBr3versus MAPbI3: suppression of methylammonium migration and reduction of halide migration. J. Phys. Chem. Lett. vol. 11 (17), 7127–7132. https://doi.org/10.1021/acs.jpclett.0c01822.
Mesquita, I., Andrade, L., Mendes, A., 2018. Perovskite solar cells: materials, configurations and stability. Renew. Sustain. Energy Rev. vol. 82 (May), 2471–2489. https://doi.org/10.1016/j.rser.2017.09.011.
Mil, S., Zinaddinov, M., Tokmoldin, N., Tokmoldin, S., 2016. Design and fabrication steps of silicon heterostructured p-i-i-n solar cell with corrugated surface. IEEE 43rd Photovolt. Spec. Conf. 342–345. https://doi.org/10.1109/PVSC.2016.7749607.
Min Nam, Y., Huh, J., Ho Jo, W., 2010. Optimization of thickness and morphology of active layer for high performance of bulk-heterojunction organic solar cells. Sol. Energy Mater. Sol. Cells vol. 94 (6), 1118–1124. https://doi.org/10.1016/j.solmat.2010.02.041.
Mohamadkhani, F., Javadpour, S., Taghavinia, N., 2019. Improvement of planar perovskite solar cells by using solution processed SnO 2 / CdS as electron transport layer. Sol. Energy vol. 191 (September), 647–653. https://doi.org/10.1016/j.solener.2019.08.067.
Nam, H.J., Jeong, S.C., Jung, D., 2008. Fabrication of textured silicon solar cell using microlens as anti-reflection layer. Conf. Optoelectron. Microelectron. Mater. Devices 2008, 246–248. https://doi.org/10.1109/COMMAD.2008.4802137.
S. Narasimha and A. Rohatgi, Fabrication and Characterization of 18.6% Efficient Multicrystalline Silicon Solar Cells, vol. 45, no. 8, pp. 1776–1783, 1998, doi: 10.1109/16.704378.
National Renewable Energy Laboratory. Best Research-Cell Efficiencies. Available online: https://www.nrel.gov/pv/assets/pdfs/best-research-cell-fficiencies.20200925.pdf (accessed on 1 July 2023).
Ouedraogo, N.A.N., et al., 2020. Stability of all-inorganic perovskite solar cells. Nano Energy vol. 67 (August 2019), 104249. https://doi.org/10.1016/j.nanoen.2019.104249.
Patil, P., Mann, D.S., Nakate, U.T., Hahn, Y.B., Kwon, S.N., Na, S.I., 2020. Hybrid interfacial ETL engineering using PCBM-SnS2 for High-Performance p-i-n structured planar perovskite solar cells. Chem. Eng. J. vol. 397 (May), 125504 https://doi.org/10.1016/j.cej.2020.125504.
Prasanna, R., et al., 2017. Band gap tuning via lattice contraction and octahedral tilting in perovskite materials for photovoltaics. J. Am. Chem. Soc. vol. 139 (32), 11117–11124. https://doi.org/10.1021/jacs.7b04981.
Protesescu, L., et al., 2015. Nanocrystals of cesium lead halide perovskites (CsPbX3, X = Cl, Br, and I): novel optoelectronic materials showing bright emission with wide color gamut. Nano Lett. vol. 15 (6), 3692–3696. https://doi.org/10.1021/nl5048779.
Qaid, S.M.H., et al., 2016. Band-gap tuning of lead halide perovskite using a single step spin-coating deposition process. Mater. Lett. vol. 164, 498–501. https://doi.org/10.1016/j.matlet.2015.10.135.
Qin, P., et al., 2014. Inorganic hole conductor-based lead halide perovskite solar cells with 12.4% conversion efficiency. Nat. Commun. vol. 5 (May), 1–6. https://doi.org/10.1038/ncomms4834.
Rahaman, M.Z., Ge, S., Lin, C.-H., Cui, Y., Wu, T., 2021. One-dimensional molecular metal halide materials: structures, properties, and applications. Small Struct. vol. 2 (4), 2000062 https://doi.org/10.1002/sstr.202000062.
Rong, Y., et al., 2017. Tunable hysteresis effect for perovskite solar cells. Energy Environ. Sci. vol. 10 (11), 2383–2391. https://doi.org/10.1039/c7ee02048a.
Rosales, B.A., Kim, J., Wheeler, V.M., Crowe, L.E., Prince, K.J., Mirzokarimov, M., Daligault, T., Duell, A., Wolden, C.A., Schelhas, L.T., Wheeler, L.M., 2023. Thermochromic halide perovskite windows with ideal transition temperatures. Adv. Energy Mater. 13, 2203331 https://doi.org/10.1002/aenm.202203331.
Seal, S., Ji, L., Budhraja, V., Varadan, V.V., 2013. Design and fabrication of a plasmonic fishnet structure for the enhancement of light trapping in thin film solar cells. IEEE 39th Photovolt. Spec. Conf. 618–620. https://doi.org/10.1109/PVSC.2013.6744226.
Shao, J.Y., Li, D., Shi, J., et al., 2023. Recent progress in perovskite solar cells: material science. Sci. China Chem. 66, 10–64. https://doi.org/10.1007/s11426-022-1445-2.
Shen, X., Kwak, S.L., Jeong, W.H., Jang, J.W., Yu, Z., Ahn, H., Park, H.J., Choi, H., Park, S.H., Snaith, H.J., Hwang, D.-H., Lee, B.R., 2023. Thermal management enables stable perovskite nanocrystal light-emitting diodes with novel hole transport material. Small 19, 2303472. https://doi.org/10.1002/smll.202303472.
Z. Shi et al., Lead-Free Organic – Inorganic Hybrid Perovskites for Photovoltaic Applications: Recent Advances and Perspectives, 2017, doi: 10.1002/adma.201605005.
Sivaprakasam, A., Elangovan, N.K., 2021. Effect of CdS thin film on the performance of methylammonium lead iodide perovskite solar cell. J. Mater. Sci. Mater. Electron. vol. 32 (13), 17612–17619. https://doi.org/10.1007/s10854-021-06294-7.
Henry J. Snaith et al., Thermally Stable Perovskite Solar Cells by All-Vacuum Deposition, 2023a, doi: 10.1021/acsami.2c14658.
Snaith, Henry J., et al., 2023b. Chloride-based additive engineering for efficient and stable wide-bandgap perovskite solar cells. vol, 2211742. https://doi.org/10.1002/adma.202211742.
Son, Y., Lee, D.Y., Choi, J.W., et al., 2016. Self-formed grain boundary healing layer for highly efficient CH3NH3PbI3 perovskite solar cells. Nat. Energy vol. 1 (7). https://doi.org/10.1038/nenergy.2016.81.
Suresh Kumar, N., Chandra Babu Naidu, K., 2021. A review on perovskite solar cells (PSCs), materials and applications. J. Mater. vol. 7 (5), 940–956. https://doi.org/10.1016/j.jmat.2021.04.002.
Tong, G., et al., 2017. Cadmium-doped flexible perovskite solar cells with a low-cost and low-temperature-processed CdS electron transport layer. RSC Adv. vol. 7 (32), 19457–19463. https://doi.org/10.1039/c7ra01110e.
Ulatowski, A.M., et al., 2020. Charge-carrier trapping dynamics in bismuth-doped thin films of MAPbBr3Perovskite. J. Phys. Chem. Lett. vol. 11 (9), 3681–3688. https://doi.org/10.1021/acs.jpclett.0c01048.
Voz, C., et al., 2012. Progress in silicon heterojunction solar cell fabrication with rear laser-fired contacts. Span. Conf. Electron Devices vol. 120000, 345–348. https://doi.org/10.1109/CDE.2013.6481413.
Wang, J., et al., 2021b. Plasma oxidized Ti3C2TxMXene as electron transport layer for efficient perovskite solar cells. ACS Appl. Mater. Interfaces vol. 13 (27), 32495–32502. https://doi.org/10.1021/acsami.1c07146.
J.T. Wang et al., Low-Temperature Processed Electron Collection Layers of Graphene/TiO 2 Nanocomposites in Thin Film Perovskite Solar Cells, 2014, doi: 10.1021/nl403997a.
Wang, K., et al., 2019b. Nano Energy Efficient perovskite solar cells by hybrid perovskites incorporated with heterovalent neodymium cations. Nano Energy vol. 61 (March), 352–360. https://doi.org/10.1016/j.nanoen.2019.04.073.
L. Wang et al., A Eu 3+ -Eu 2+ ion redox shuttle imparts operational durability to Pb-I perovskite solar cells, vol. 270, no. January, pp. 265–270, 2019c.
Wang, M., Feng, Y., Bian, J., Liu, H., Shi, Y., 2018a. A comparative study of one-step and two-step approaches for MAPbI3 perovskite layer and its influence on the performance of mesoscopic perovskite solar cell. Chem. Phys. Lett. vol. 692, 44–49. https://doi.org/10.1016/j.cplett.2017.12.012.
Wang, M., Zang, Z., Yang, B., Hu, X., Sun, K., Sun, L., 2018b. Performance improvement of perovskite solar cells through enhanced hole extraction: The role of iodide concentration gradient. Sol. Energy Mater. Sol. Cells vol. 185 (May), 117–123. https://doi.org/10.1016/j.solmat.2018.05.025.
Wang, R., et al., 2019a. Caffeine improves the performance and thermal stability of perovskite solar cells. Joule vol. 3 (6), 1464–1477. https://doi.org/10.1016/j.joule.2019.04.005.
Wang, S., Yousefi Amin, A.A., Wu, L., Cao, M., Zhang, Q., Ameri, T., 2021a. Perovskite nanocrystals: synthesis, stability, and optoelectronic applications. Small Struct. vol. 2 (3), 2000124 https://doi.org/10.1002/sstr.202000124.
Wang, Y.Z., Hou, R., 2021. Fabrication strategy to promote performance of perovskite solar cells. J. Phys. Conf. Ser. vol. 2109 (1) https://doi.org/10.1088/1742-6596/2109/1/012007.
Z. Wang, M. Li, Y. Yang, Y. Hu, H. Ma, and X. Gao, High Efficiency Pb – In Binary Metal Perovskite Solar Cells, 2016, doi: 10.1002/adma.201600626.
Wheeler, L.M., et al., 2017. Switchable photovoltaic windows enabled by reversible photothermal complex dissociation from methylammonium lead iodide. Nat. Commun. 8, 1722.
Wieghold, S., et al., 2018. Precursor concentration affects grain size, crystal orientation, and local performance in mixed-ion lead perovskite solar cells. ACS Appl. Energy Mater. vol. 1 (12), 6801–6808. https://doi.org/10.1021/acsaem.8b00913.
Wu, X., et al., 2016. Two-dimensional modeling of TiO2 nanowire based organic-inorganic hybrid perovskite solar cells. Sol. Energy Mater. Sol. Cells vol. 152, 111–117. https://doi.org/10.1016/j.solmat.2016.03.017.
Wu, Y., Li, X., Zeng, H., 2021. Lead-free halide double perovskites: structure, luminescence, and applications. Small Struct. vol. 2 (3), 2000071 https://doi.org/10.1002/sstr.202000071.
Z. Xiao, Z. Song, and Y. Yan, From Lead Halide Perovskites to Lead-Free Metal Halide Perovskites and Perovskite Derivatives, vol. 1803792, pp. 1–22, 2019, doi: 10.1002/adma.201803792.
Xie, F., et al., 2017. Vertical recrystallization for highly efficient and stable formamidinium-based inverted-structure perovskite solar cells. Energy Environ. Sci. vol. 10 (9), 1942–1949. https://doi.org/10.1039/c7ee01675a.
W. Xu et al., Efficient Perovskite Solar Cells Fabricated by Co Partially Substituted Hybrid Perovskite, vol. 1703178, pp. 1–11, 2018, doi: 10.1002/aenm.201703178.
Xu, X., Wang, X., 2020. Perovskite nano-heterojunctions: synthesis, structures, properties, challenges, and prospects. Small Struct. vol. 1 (1), 2000009 https://doi.org/10.1002/sstr.202000009.
Yamada, Y., Nakamura, T., Endo, M., Wakamiya, A., Kanemitsu, Y., 2014. Photocarrier recombination dynamics in perovskite $CH_3NH_3PbI_3$ for solar cell applications. J. Am. Chem. Soc. vol. 136 (33), 11610–11613. https://doi.org/10.1021/ja506624n.
Yang, D., et al., 2018. High efficiency planar-type perovskite solar cells with negligible hysteresis using EDTA-complexed SnO2. Nat. Commun. vol. 9 (1) https://doi.org/10.1038/s41467-018-05760-x.

Yang, Y., et al., 2015. The size effect of TiO2 nanoparticles on a printable mesoscopic perovskite solar cell. J. Mater. Chem. A vol. 3 (17), 9103–9107. https://doi.org/10.1039/c4ta07030e.

Yin, Y., et al., 2020. Efficient and stable ideal bandgap perovskite solar cell achieved by a small amount of tin substituted methylammonium lead iodide. Electron. Mater. Lett. vol. 16 (3), 224–230. https://doi.org/10.1007/s13391-020-00206-3.

You, J., et al., 2016. Improved air stability of perovskite solar cells via solution-processed metal oxide transport layers. Nat. Nanotechnol. vol. 11 (1), 75–81. https://doi.org/10.1038/nnano.2015.230.

Zhang, J., et al., 2016. N-type doping and energy states tuning in CH3NH3Pb1-xSb2x/3I3 perovskite solar cells. ACS Energy Lett. vol. 1 (3), 535–541. https://doi.org/10.1021/acsenergylett.6b00241.

J. Zhang, R. Chen, Y. Wu, M. Shang, Z. Zeng, and Y. Zhang, Extrinsic Movable Ions in MAPbI 3 Modulate Energy Band Alignment in Perovskite Solar Cells, vol. 1701981, pp. 1–8, 2017, doi: 10.1002/aenm.201701981.

Zhang, L., et al., 2015. The effect of carbon counter electrodes on fully printable mesoscopic perovskite solar cells. J. Mater. Chem. A vol. 3 (17), 9165–9170. https://doi.org/10.1039/c4ta04647a.

Y. Zhang *et al.*, N-type Doping of Organic-Inorganic Hybrid Perovskites Toward High-Performance Photovoltaic Devices, vol. 1800269, pp. 1–9, 2019, doi: 10.1002/solr.201800269.

Zhao, P., Kim, B.J., Jung, H.S., 2018. Passivation in perovskite solar cells: a review. Mater. Today Energy vol. 7, 267–286. https://doi.org/10.1016/j.mtener.2018.01.004.

Zhao, W., Yao, Z., Yu, F., Yang, D., Liu, S.F., 2017. Alkali metal doping for improved CH3NH3PbI 3 perovskite solar cells, vol. 1700131, 1–7. https://doi.org/10.1002/advs.201700131.

Zhao, Y., Zhu, K., 2015. Three-step sequential solution deposition of PbI2-free CH3NH3PbI3 perovskite. J. Mater. Chem. A vol. 3 (17), 9086–9091. https://doi.org/10.1039/c4ta05384b.

Zheng, J., et al., 2022. Effects of the incorporation amounts of CdS and Cd(SCN2H4)2Cl2 on the performance of perovskite solar cells. Int. J. Miner. Metall. Mater. vol. 29 (2), 283–291. https://doi.org/10.1007/s12613-021-2316-0.

Zhou, D., Zhou, T., Tian, Y., Zhu, X., Tu, Y., 2018. Perovskite-based solar cells: materials, methods, and future perspectives. J. Nanomater. 2018 https://doi.org/10.1155/2018/8148072.

Zhou, Z., Qiang, Z., Sakamaki, T., Takei, I., Shang, R., Nakamura, E., 2019. Organic/inorganic hybrid p-type semiconductor doping affords hole transporting layer free thin-film perovskite solar cells with high stability. ACS Appl. Mater. Interfaces. https://doi.org/10.1021/acsami.9b06513.

Zhu, H., Teale, S., Lintangpradipto, M.N., et al., 2023. Long-term operating stability in perovskite photovoltaics. Nat. Rev. Mater. 8, 569–586. https://doi.org/10.1038/s41578-023-00582-w.

Zimmermann, E., et al., 2016. Characterization of perovskite solar cells: towards a reliable measurement protocol. APL Mater. vol. 4 (9) https://doi.org/10.1063/1.4960759.